*Coordination Chemistry Reviews*, 29 (1979) 1—66



# VIBRATIONAL STUDIES OF SOLID INORGANIC AND COORDINATION COMPLEXES AT HIGH PRESSURES *

JOHN R. FERRARO

*Chemistry Division, Argonne National Laboratory, Argonne, Illinois 60439 (U.S.A.)*

(Received 1 December 1978)

CONTENTS



## A. INTRODUCTION

The earliest high-pressure studies were made by Amagat [1], but the important and fundamental studies on high pressure were conducted by Bridgman [2—16] who has been called the father of high-pressure chemistry. Bridgman

* Work performed under the auspices of the Division of Basic Energy Sciences of the U.S. Department of Energy. Based on a series of lectures presented at the Universities of Florence and Rome, Italy, May 1978, as Visiting Professor of the Italian Consiglio Nationale della Ricerche and as NATO recipient of a 1978 Senior Scientist Fellowship Award.

was able to attain pressures to $10^5$ atm. His work still finds extensive use today, and his compressibility data as a function of pressure for common liquids was a classical achievement.

There are several books and reviews [3,17—26] on high pressure, some of which cover the history of high pressure comprehensively. It is not intended in this review article to dwell on the history of high pressure to any large degree for fear of being redundant with already published material.

The general effects of pressure on matter have been discussed by Sinn [26].

It is the aim of this review to discuss the effects of pressure to 150 kbar on the vibrational transitions occurring in solid materials such as inorganic compounds and coordination complexes. The magnitudes of these effects are measured by IR and Raman scattering methods. The review restricts itself chiefly with the versatile diamond anvil cell. Electronic transitions have been discussed by Drickamer and Frank [27].

*(i) Units of pressure*

A brief discussion on the units of pressure is necessary at this point. The international standard (SI) unit of pressure is the Pascal or Newton per square meter. The interrelationships between various units in use today and the SI units are given as follows

1 bar = $10^5$ N $m^{-2}$ (or Pascal) = $10^6$ dyne $cm^{-2}$ = 0.9869 atm = 1.0197 kg $cm^{-2}$

1 atm = $1.01325 \times 10^6$ dyne $cm^{-2}$

We will use kbar in this discussion, which corresponds to $10^3$ bar, and at extremely high pressures, Mbar, where 1 Mbar = $10^3$ kbar.

To provide the newcomer with an idea of the magnitude of some of these pressure values, Table 1 has been compiled.

TABLE 1

Naturally occurring pressures [26]

| Pressure (kbar) | Site of occurrence |
|---|---|
| 1 | Deepest part of ocean — Marianas trench |
| 10. | Crust—mantle interface — Mohorovicic discontinuity |
| $1.37 \times 10^3$ | Mantle—core interface — Wichert-Gutenburg discontinuity |
| $3.64 \times 10^3$ | Center of earth |
| $1 \times 10^8$ | Center of sun |
| $10^{10}$—$10^{14}$ | White dwarf star |
| $10^{17}$—$10^{21}$ | Neutron stars |

## B. INSTRUMENTATION FOR OPTICAL MEASUREMENTS AT HIGH PRESSURES [28]

The instrumentation necessary to make spectroscopic measurements at non ambient pressures includes an optical high pressure cell, a spectrophotometer, and the interface or optical link of the cell with the spectrophotometer. The optical link of the pressure cell to an IR spectrophotometer necessitates the use of a beam condenser, and to an interferometer a light-pipe or a beam condenser may be necessary. Very important considerations of this instrumentation are the windows used in the optical high pressure cell. The properties of the windows are of prime importance since they must be transparent to the electromagnetic radiation of interest and must be of sufficient strength to withstand high pressures. Ancillary equipment for some systems may include pressure-transmitting and pressure-measuring devices.

### *(i) Optical high pressure cells*

The high pressure cells which can be used for optical purposes may be of three main types: (1) shock wave cell; (2) piston-cylinder cell; and (3) opposed anvil cell. Table 2 summarizes advantages and disadvantages of the three types of cells.

#### *(1) Shock wave cell*

The shock wave cell utilizes high explosives to obtain pressure and will give the highest pressures of any cell discussed in this paper [29]. However, the pressures are of short duration and may be destructive to the sample and optical equipment; moreover making the optical link to a spectrophotometer is difficult. Since the effects of pressure are of short duration ($10^{-5}$ s) fast-scanning spectrophotometers are necessary. Except in specialized cases where extreme pressures are necessary to demonstrate some phenomenon, the shock wave cell and technique are less practical than the piston-cylinder or the opposed anvil cell. Many of the physical measurements that are possible with the latter two cells on in situ samples are not possible with shock-waves.

#### *(2) Piston-cylinder cell*

The piston-cylinder type cell or variations thereof have made notable contributions and can be used in an extended region of the electromagnetic spectrum from the UV region to the IR. The piston-cylinder cell has been used primarily for solids, although it has been adapted for use with liquids or solutions as well.

The best known cell of this type is the supported taper Drickamer cell, which was developed by Drickamer and his students [30—33], and is a cross between an anvil and a piston-cylinder apparatus. Several variations of this cell have now been made. Tables 3 and 4 summarize details of the pressure

TABLE 2

Types of optical high pressure cells

| Type of cell | Pressure (kbar) | Advantages | Disadvantages |
|---|---|---|---|
| Shock wave | >>1000 | 1. Highest obtainable pressures | 1. Pressure exerted over short time<br>2. May be destructive to optical equipment and sample<br>3. High explosives needed to obtain shock wave |
| Piston and cylinder [a] | 180 | 1. Largest specimen volume<br>2. Gives more nearly hydrostatic pressures<br>3. Can be used for liquids or solutions | 1. Insufficient optical clarity to permit microscopic observation or photography of sample<br>2. Specimen may interact with salt matrix<br>3. Difficult to use |
| Opposed anvils (diamonds) | 1700 | 1. Only micro quantities of material necessary.<br>2. Compact — can be used with spectrophotometers and microscope easily<br>3. Can use for liquids or solutions<br>4. No matrix interference | 1. Pressure gradient exists in cell<br>2. Absorption of diamonds may be troublesome<br>3. Cannot use large specimen of solids |

[a] Or modifications thereof.

cells that are in use for optical studies of solids and liquids or solutions.

The piston-cylinder cell is considered to give essentially hydrostatic pressures, an important consideration in pressure studies. The Drickamer cell has two versions, one capable of providing pressures up to 60 kbar and the other to 200 kbar. Figure 1 shows the design of one of these cells. The pressure is exerted perpendicular to the light path. Sodium chloride serves as the spectroscopic window and the pressure-transmitting fluid.

The sample is loaded into the center of a small disc of NaCl. Although the cell accommodates the largest possible sample specimen for pressure measurements, the sample is surrounded by a salt matrix. If one wishes to study pressure effects on ionic solids, this could present a problem. Additionally, the hygroscopic nature of the salt matrix is detrimental. Other materials besides NaCl may be substituted for the center disc. This has the disadvantage in that it would shorten the life of the NaCl windows, and the matrix problem would always exist.

TABLE 3

Piston-cylinder cell (solids)[a]

| Pressure limits (kbar) | Optical instrument | Windows | Wavelength range (μm) | Remarks | Ref. |
|---|---|---|---|---|---|
| 160 | Beckman DU (0.25—10 μm), Perkin-Elmer single beam, double prism instrument in IR | NaCl | UV, Visible NIR, MIR to 10 | Sapphire, $CaF_2$ windows have also been used; 80—450 K | 30—33 |
| 30 | Beckman | Quartz, sapphire | 0.36—0.40 | | 36 |
| 30[c] | IKS-12 | Diamond | 5—6 | | 37 |
| 55 | RIIC, Grubb-Parsons Cube interferometer | Sapphire, diamonds (type II) MgO, fused silica, Irtran | 1—1000 | 77—500 K[64,65] | 35 |
| 10—20[c,d] | Perkin-Elmer | Sapphire | 1—5 | 2—300 K | Vu[b] |
| | Coderg | Diamond | 100—1000 | | |
| 9 | RIIC 720FS interferometer and *f*-2 single pass grating instrument of Ebert type | Quartz | 90—500 | For FIR, hydrostatic gas pressure cell | 38[b] |
| 50 | PE 421, 400, JACO | NaCl | | 77—500 K | 46[b] |

[a] Abbreviations: NIR, near infrared; MIR, mid-infrared; FIR, far infrared. [b] Personal communication. [c] Can be used for liquids as well. [d] Can be used for gases as well.

TABLE 4

Piston-cylinder cells (liquids or solution)

| Pressure limits (kbar) | Optical instrument | Windows | Wavelength range ($\mu$m) | Remarks | Ref. |
|---|---|---|---|---|---|
| 200 [a] | Perkin-Elmer model 521 | KBr or NaCl | 5—6 | Used to study carbonyl reactions in metal carbonyls | 39 |
| 40 | Beckman DK-2 | Sapphire | 0.2—0.33 | Solutions of inorganic salts in $H_2O$ | 40 |
| 10—12 | Perkin-Elmer model 112 | Sapphire | 0.2—5 | Studied $\nu_{OH}$ band in butanol solutions of $CS_2$ | 41 |
| 1.5<br>10 | Beckman IR-5A [b] | Irtran 1 or 2 | ~6 | Study of C≡C vibration | 42 |
| 12 [c] | (?) | Sapphire | 3 | Studies of $H_2O$ | 43 |
| 1 | (?) | Sapphire | (?) | Cell claimed to be suitable for use to 6 kbar | 44 |

[a] Can be used to 373 K. [b] With grating monochromator. [c] Similar to Drickamer cell in Table 3.

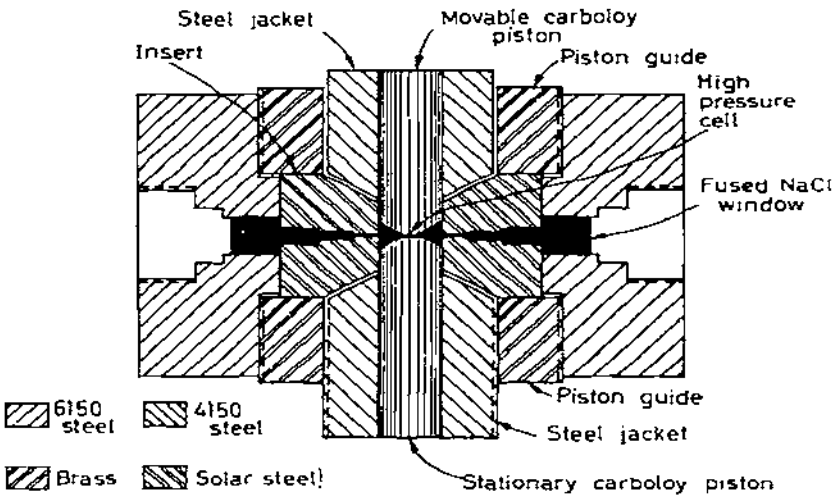


Fig. 1. Drickamer cell used for high pressure optical measurements [30—33]. (Figure reproduced through the courtesy of the authors and John Wiley and Sons, Inc., New York.)

The use of this cell requires a high degree of expertise and further requires high precision machine shop facilities to construct it. The cell has been used for pressure applications of 180 kbar at 773 K [34] and 55 kbar at 77 K [35]. The cell has been modified to be used for liquids or solutions [41,43]. The Drickamer cell or modifications thereof have also been used for Raman measurements at high pressures [45,46]. This application will be discussed in a later section. A Drickamer-type apparatus for pressures to 400 kbar has been reported [47].

*(3) Anvil-type cell*

Perhaps the most versatile pressure cell that has been used for optical studies has been the diamond anvil cell (DAC), as developed by Weir and associates [48]. Figure 2 shows the details of this cell. The diamonds serve as the pressure transmitting material as well at the windows. Pressures close to 100 kbar, depending on the size of the diamonds, are routinely reached. However, the DAC has been used with pressure as high as 300 kbar [49], and conceivably smaller diamonds could generate even higher pressures. The cell can be used for solutions or liquids, although a gasket is necessary for this application. Figure 3 illustrates a gasketing technique used with liquids [50]. The

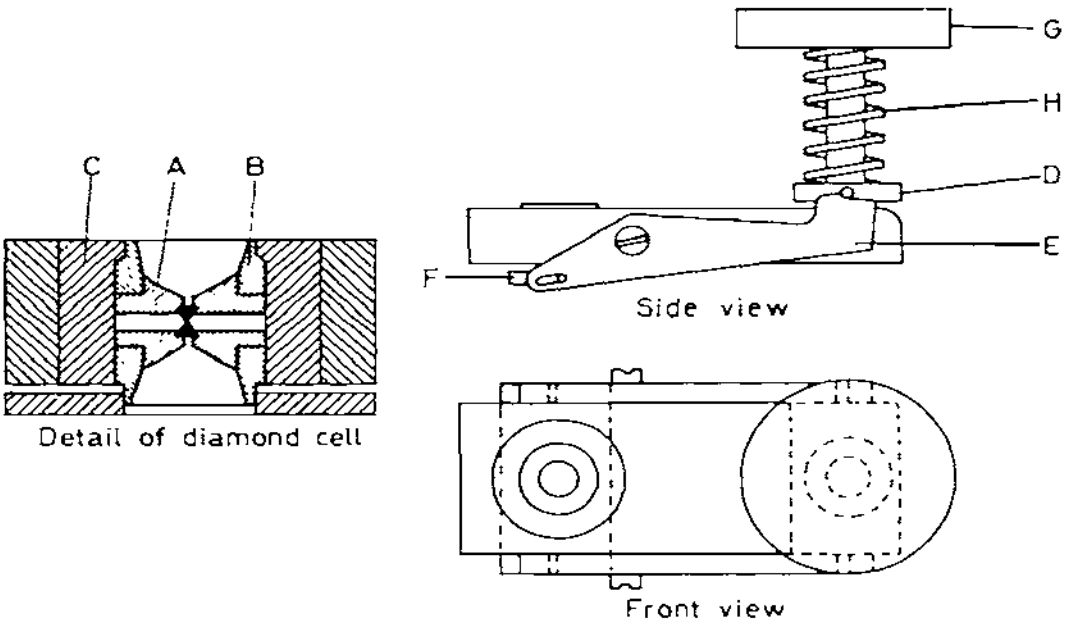


Fig. 2. Diamond anvil high pressure optical cell. A and B, parts of pistons; C, hardened steel insert; D, pressure plate; E, lever; G, screw; H, calibrated spring. (Figure reproduced through the courtesy of the authors and Applied Spectroscopy.)

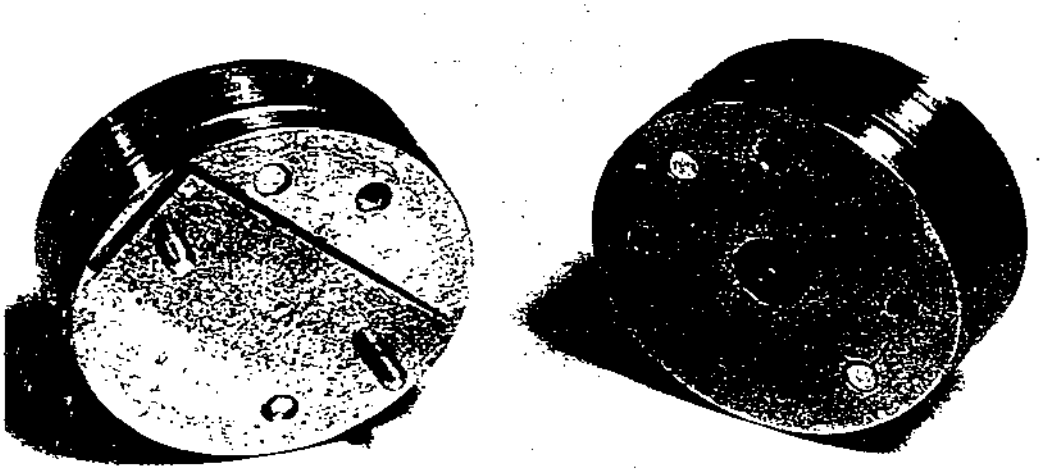

Fig. 3. A gasket technique with DAC [50]. (Figure reproduced through the courtesy of the authors and Applied Spectroscopy.)

DAC has also been used at temperatures of ca. 3000 K [51] and cooled down to liquid nitrogen temperatures [52].

Recently improved versions of the DAC were developed [53,54], and Fig. 4 illustrates the details of the modifications used by Adams and Payne. Pressure in this cell is applied through a small hydraulic ram instead of the calibrated screw of the original version. The other improved version of the DAC is the Waspaloy cell [54]. Figure 5 shows the essential parts of the design. The diamond alignment is improved from the original design. One diamond is mounted in a hemisphere, while the other diamond is mounted on a plate which is translationally positioned for axial alignment by screw adjustments. A loose fitting heating coil is placed in the cell. The cell can be used with gaskets for hydrostatic pressure to 100 kbar, and has been used to 973 K and 200 kbar pressure.

An ultrahigh pressure diamond cell has now been developed [55], and megabar pressures can be generated. The cell is made of hardened (RWC-55) 4340 alloy steel. For high temperature studies the cell can be made from Inconel. Mao and Bell [56] have described an ultrahigh-pressure diamond cell, which they claim to have used to 1.7 Mbar [57]. These new ultrahigh pressure cells now make experiments simulating geochemical reactions in the mantle of the earth possible.

One shortcoming of the DAC is the lack of hydrostatic pressure across the diamond faces. This pressure gradient, which may demonstrate pressures 1.5 times greater at the center than the edges [58], may not be entirely disadvantageous. However, with the use of a gasket and a pressure transmitting fluid the

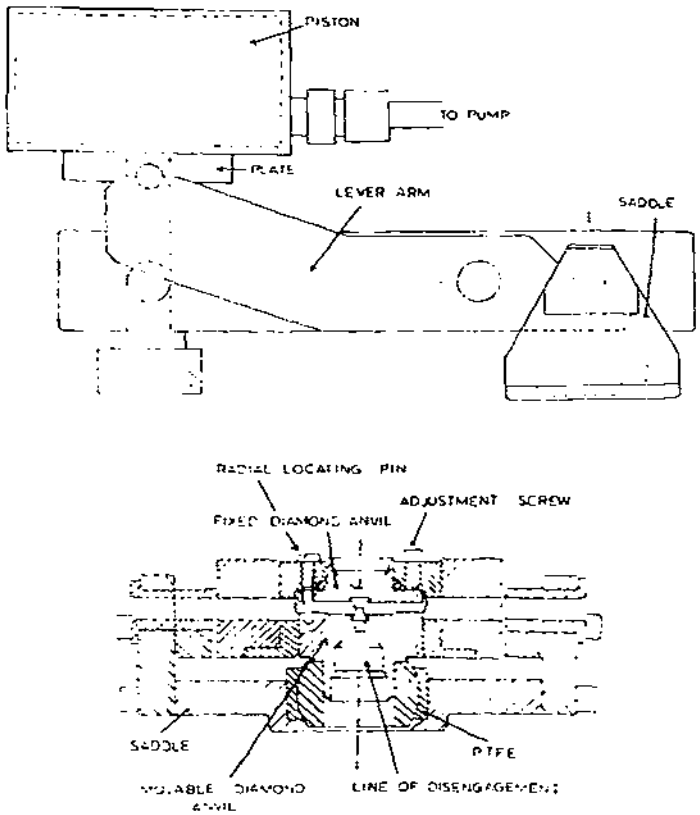


Fig. 4. Modified DAC cell [53]. (Figure reproduced through the courtesy of the authors and Applied Spectroscopy.)

the problem of non-hydrostatic pressure can be circumvented. Phase changes may be readily identified in the DAC, using a microscope, by the change in color occurring and the sharp demarcation between phases. Color changes alone, particularly in coordination compounds, do not necessarily indicate a phase change. A primary requisite is the appearance of the Becke line of demarcation. In colorless materials, the phase changes may be identified by the Becke line, which demarcates the phases. The DAC is compact and can be readily used with a microscope. All loadings of solid materials into the DAC should be monitored microscopically to ensure a proper distribution in the cell. This procedure prevents any diamond—diamond contact, which could cause chipping or gouging of the diamonds. Additionally, such monitoring can alert the experimenter to any phase change or other phenomena occurring.

The DAC has also been used for Raman work at high pressures, and this instrumentation will be discussed later [53,59—61].

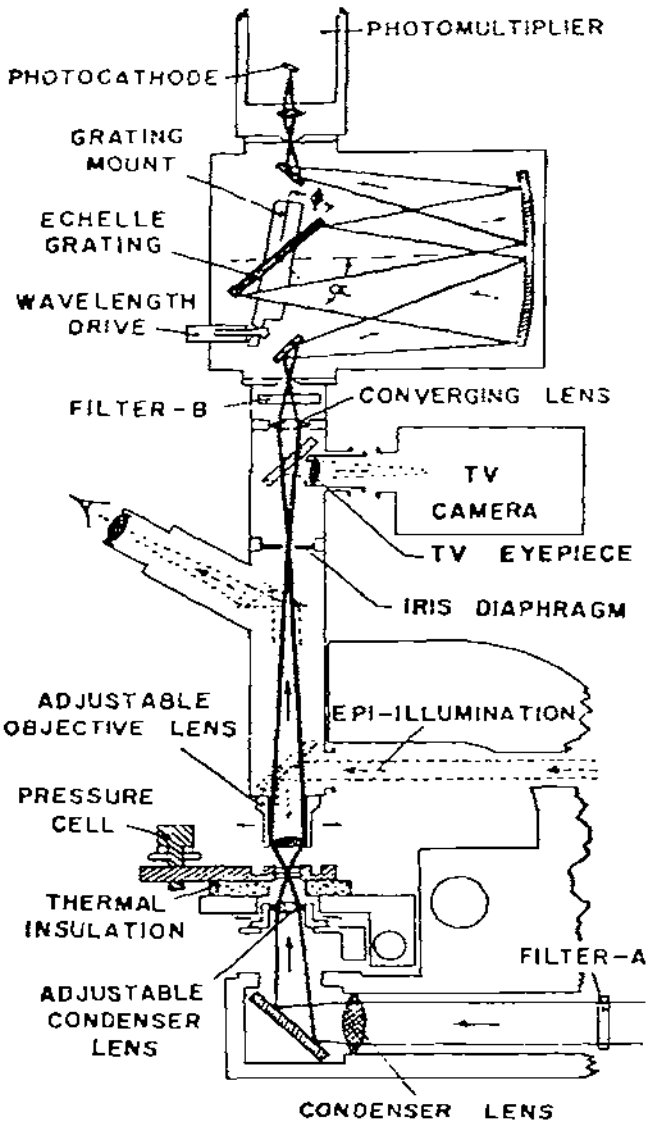


Fig. 5. Details of the Waspaloy pressure cell [54]. (Figure reproduced through the courtesy of the authors and Review of Scientific Instruments.)

Table 5 summarizes the details of some of the anvil cells that are in use for optical studies.

*(ii) Optical link of pressure cell with spectrophotometer or interferometer*

Owing to the small optical aperture in the DAC (ca. 0.25 $mm^2$ in area or larger) and in the piston-cylinder cell (Drickamer cell I, 0.028 in. and cell II,

TABLE 5

Anvil-type pressure cells (solids) used for optical spectroscopy [a]

| Pressure limits (kbar) [b] | Optical Instrument | Windows | Wavelength range (μm) | Remarks | Ref. |
|---|---|---|---|---|---|
| 100 | Perkin-Elmer models 421, 350, Beckman IR-4 | Diamond [c,d] | 2—35 | 6 × beam condenser | 48 |
| 200 | Perkin-Elmer models 225, 350, FTS-14 | Diamond | 0.27—40 | 6 × beam condenser | 62, 63 |
| 100 | Perkin-Elmer model 301 | Diamond | 16—200 | 6 × beam condenser | 64 |
| 100 | Beckman IR-11 | Diamond | 16—200 | 6 × beam condenser | 65 |
| 100 | Beckman IR-12 | Diamond [d] | 2.5—16 | 6 × beam condenser | 65 |
| 100 | Cary-14 | Diamond | 0.25—2.5 | With or without a beam condenser | 66 |
| 100 | Digilab FTS 20 A | Diamond | 1—1000 | With beam condenser | 68 |
| 100 | Beckman FS-520 interferometer | Diamond | FIR → 250 | Light pipe necessary | 67 |
| 100 | Beckman #4260 | Diamond [d] | 2—50 | With beam condenser | 69 |
| 35 | Michelson Interferometer | Quartz | | Cube-anvil type cell | 70 |
| 50 [f] | (?) | Diamond | NIR | Cube-anvil type cell; sample contained in NaCl; uses quartz or sapphire for lower pressures | 71 |
| 150 | FTS-14 | Diamond | 2.5—200 | 298—673 K | e(1) |
| 200 | PE 421, 210, Cary 14R, Spex 1700 | Diamond | 0.2—40 | To 973 K | e(2) |
| | FTS-14 | Diamond | 2.5—500 | | e(3) |
| 10 | Cary 14R | Diamond | 0.19—5 | 123—623 K | e(4) |
| 100 | Perkin-Elmer model 225 | Diamond | | Refracting beam condenser | 73 |

[a] DAC can be used for liquid or solutions if a gasket is used between the anvils. [b] DAC can be used routinely to 100 kbar if diamonds are properly aligned. [c] Diamond-Type I has absorptions at 3 μm (weak), 4—5.5 μm (intense), 7—10 μm (intense); Type II has absorptions at 3 μm (weak), 4—5.5 μm (intense). [d] Sapphire windows may be used from 2—5 μm. [e] Personal communication: (1) R.J. Jakobsen, Battelle Memorial Inst.; (2) G.J. Piermarini, Nat. Bur. Stand.; (3) G. Carlson, Westinghouse, Pittsburgh, Pa.; (4) C.A. Angell, Purdue Univ. [f] Claimed to be used to 1273 K.

0.037 in.) a means of condensing the source beam becomes necessary. In the case of a grating double beam spectrophotometer a beam condensation process is used (usually from 4—6× condensation) [48,62—66]. In the case of interferometric measurements a light-pipe has been used both for the entrance energy and the exit energy in the far IR region [67]. Recently, a new Harrick 6× beam condenser has been interfaced with the Digilab 20A interferometer [68]. A 4× beam condenser has also been coupled with a Beckman Model no. 4260 [69].

Using diamonds as the optical windows puts a stringent requirement on the properties of the beam condenser. The critical angle of diamonds is 26°. As a result the beam condenser should condense the light in a cone having an angle less than 52°. Also, since the faces of the diamonds are so small, the spot size of the condensed light should be as small as feasible, 1 $mm^2$ or less. One can then be sure that most of the condensed light is reaching the sample between the two diamonds and is not clipped by the large size of the DAC. Adams and Sharma [73] have recently reported a refracting beam condenser for IR use with the DAC. The optical problems associated with IR spectroscopy with a DAC are discussed [73].

For Raman scattering experiments both the DAC and the piston-cylinder may be used without any condensation of source energy, since lasers are used as the exciting sources with narrow beam radii. The laser light can be focussed directly into the small optical aperture of the pressure cell without too much difficulty.

*(iii) Instrumentation for Raman spectroscopy at high pressure*

Both the piston-cylinder and anvil-type cells have been used for obtaining Raman spectra at high pressure. Although energy problems are severe in IR spectroscopy because of the small optical aperture in the high pressure cells, the advent of laser sources for Raman spectroscopy has overcome a great deal of these problems.

The first Raman spectra obtained in a DAC were made in 1968 [59,60]. The red → yellow transition in $HgI_2$ followed. In both cases 0° scattering geometry was used, although it was cited that 180° scattering could be used [59]. The DAC was also used for the study of liquid $Br_2$ and $CS_2$ [61]. However, except for solids with high Raman scattering efficiencies, the final results were disappointing. Recently, the DAC has been used with certain modifications and with improved results [53]. Adams et al. used a tungsten carbide window in place of one of the diamonds in the DAC [53]. The details are illustrated in Fig. 6. Both 90° and 180° scattering geometries were used. One limitation is that the tungsten carbide limits the maximal pressures to ca. 30 kbar. The tungsten carbide allows the Raman intensity to build up by allowing the excitation energy to traverse twice through the sample and additionally acts as a mirror. It has been suggested that back-silvering of one diamond anvil would give comparable results in the DAC and allow the DAC to be used

TABLE 6

Pressure cells used in Raman spectroscopy

| Type of cell | Optical instrument | Pressure limits (kbar) | Temp. limits (K) | Windows | Remarks | Ref. |
|---|---|---|---|---|---|---|
| Opposed anvil | Spex 1401 | 100 | 77—350 | Diamond | Solids | 59 |
| Drickamer | Spex 1401 | 100 | 77—350 | Diamond | Solids | 45 |
| Opposed anvil | Spex 1401 Cary 81 | 200 | 573 | Diamond | Solids, liquids | 60, 61 |
| Hydrostatic gas pressure | Spex 1401 | 9 | 77—290 | Sapphire, quartz | Solids, gases | 38 |
| Waspaloy (opposed anvil) | Spex 1401 | 200 | to 973 | Diamond | Solids, liquids, solutions | 54 |
| Drickamer | Spex 1400 | 100 | 4—1300 | NaCl, diamond | Solids, liquids solutions | 46 |
| Daniels | Spex 1400 | 10 | R.T. | Sapphire | Solids | 79 |
| Sapphire, back-scattering | Cary 81 | 11 | 473—573 | Sapphire | Solutions, solids, liquids | 80, 81 |
| Piston-cylinder | Jarrell-Ash | ≤3 | | Sapphire | Solutions, liquids | 82 |
| Piston-cylinder | Coderg | 10 | 2—300 | Sapphire | Solids, liquids, solutions, gases | 83 |
| Opposed anvil | Coderg | 30 | | Diamond, sapphire | Solids | 53, 74 |
| Daniels | Spex 1401 | 10 | 77—400 | Sapphire | Solids, liquids, and Brillouin spectra | 84—86 |
| Piston-cylinder | Spex 1401 | 7 | 1.4 to R.T. | Sapphire | Solids | 87 |
| Pressure vessel | Jarrell-Ash | 220 | 100—700 | Diamond | Solids, liquids, solutions | 88 |
| Special cell | Spex 1405 | 3 | 223—473 | Quartz | Liquids, gases | 89 |
| Drickamer | Cary 81 | 55 | 77—500 | Sapphire | Solids | [a] |

[a] Personal communication with W.F. Sherman, Physics Department, King's College, University of London, Strand, London WC2R 2L5, Gt. Britain.

TABLE 7

High pressure in optical materials[a]

| Material | Spectral range (μm) | Refractive index[b] at λ (μm) | Modulus of rupture[b] (p.s.i.) | Young's modulus[b] (p.s.i.) | Compressive strength (p.s.i.) | Hardness Knoop No. | Solubility (g/100 g $H_2O$) |
|---|---|---|---|---|---|---|---|
| NaCl | 0.2—15 | 1.52 at 4<br>1.4 at 10 | | $5.8 \times 10^6$ | | 15.2—18.2 | 35.7(0°C) |
| Lithium fluoride, LiF | 0.11—6 | 1.35 at 4<br>1.1 at 10 | | $9.40—11 \times 10^6$ | | 102—113 | 0.27(18°C) |
| Irtran 1, $MgF_2$ | 1—8 | 1.35 at 4 | 21 800 | $16.6 \times 10^6$ | 157 600 | 576 | 0.0076 (18°C) |
| Calcium fluoride, $CaF_2$ | 0.13—9 | 1.41 at 4 | | $11—15 \times 10^6$ | | 158 | 0.0016 (18°C) |
| Irtran 3, $CaF_2$ | 1—10 | 1.41 at 4<br>1.34 at 8.3 | 5 300 | $14.3 \times 10^6$ | | 200 | Insoluble |
| Irtran 2, ZnS | 2—14 | 2.25 at 4<br>2.20 at 10 | 14 100 | $14 \times 10^6$ | 121 200 | 354 | 0.00069 (18°C) |
| Irtran 4, ZnSe | 0.5—20 | 2.5 at 4<br>2.4 at 10 | 6 100 | $10.3 \times 10^6$ | | 150 | Insoluble |
| Magnesium oxide, MgO | ≤6.8 | 1.7 at 2.2<br>1.66 at 4.3 | | $3.6 \times 10^6$ | | 690—692 | 0.000012 |
| Irtran 5, MgO | 1—8 | 1.67 at 4<br>1.60 at 6 | 19 200 | $48.2 \times 10^6$ | | 640 | 0.00062 |

| | | | | | |
|---|---|---|---|---|---|
| Sapphire, $Al_2O_3$ | ≤5.5 | 1.73 at 2.2 | $50.56 \times 10^6$ | 1370<br>1525—2000 | $9.8 \times 10^{-5}$ |
| Diamond * | [c] | | | | |
| Type I | 2—4, 5.5—7, 10—16 | 2.4173 | | 7000 | Insoluble |
| Type II | 0.26—4; 5.5 through FIR | | | | |
| Ceramic barium titanate, $BaTiO_3$ | ≤6.9 | 2.4 at 2.2, 4.3 | $16.50 \times 10^6$ | | |
| Calcite, $CaCO_3$ | 0.2—5.5 | ≈1.7 | | | |
| Germanium | 1.8—2.3 | ≈4.0 | | | |
| Silicon | 1—9 | 3.43<br>3.42 | | | |
| Fused silica $SiO_2$ (Corning 7905, GE type 101-100, Infrasil) | 0.3—3.5 | 1.43 | | | |
| NBS F158 $SiO_2$ | 4.5 | 1.80 | | | |
| Bausch & Lomb [d] | | | | | |
| RIR-2 | 4.5 | 1.75 | | | |
| RIR-10, 11, 12 | 5.0 | 1.62 | | | |
| RIR-20 | 5.5 | 1.82 | | | |

* Diamond has the highest Debye temperature and type II diamonds demonstrate higher thermal conductivity than type I diamonds (see C.Y. Ho, R.W. Powell and P.E. Lilly, J. Phys. Chem. Ref. Data, Supp. 1, 3 (1974) L-118. [a] Taken in part from ref. 72. [b] 298 K. [c] UV and visible absorption and FIR depend upon particular type of diamonds used here. [d] Calcium aluminate ($CaO—Al_2O_3$) and similar materials. [e] Note that UV limitations exist for all of these materials in addition to those of diamonds.

with both diamonds. An improved method for coupling the DAC optically with a Raman spectrometer has been discussed by Adams et al. [74]. The fluorescence problem of diamonds under laser excitation and its effects on the Raman measurements in a DAC are discussed by Adams and co-workers [53,72,75].

The first high pressure Raman study with a piston-cylinder cell was made by Gonikberg and co-workers [76]. A Raman study using a piston-cylinder cell (Daniel type) which gives hydrostatic pressure has been made [77—79]. Figure 7 illustrates this cell. Walrafen used a back-scattering Raman cell equipped with windows made of single crystals of sapphire [80]. Nicol et al. [46] and Ferraro [45] have used the Drickamer cell for Raman studies.

Table 6 summarizes the various pressure cells used for Raman spectroscopy at high pressures.

*(iv) Optical windows for use at high pressures*

For the anvil-type high pressure cells the window material serves the dual purpose of transmitting the pressure and being transparent to the electromagnetic radiation of interest. In the Drickamer piston-cylinder cell this is also true in part, although the mechanism of pressure transmission is not done by the window. Table 7 lists a number of possible windows for use at high

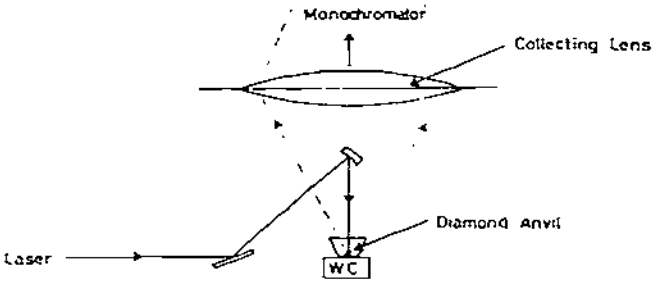


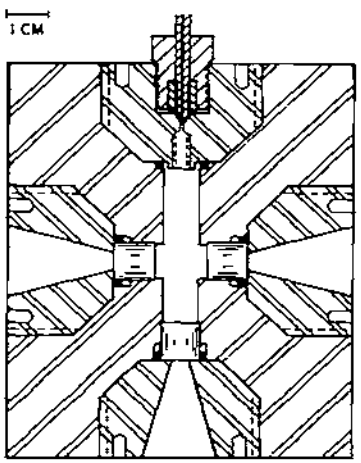


Fig. 6. Details of DAC with one tungsten carbide anvil [53]. (Figure reproduced through the courtesy of the authors and Applied Spectroscopy.)

Fig. 7. Daniels-type Raman cell [77—79]. High pressure optical cell with three oriented single crystal synthetic sapphire windows. The *C* axes of the sapphire windows are oriented normal to the flat window faces. (Figure reproduced through the courtesy of the authors and Review of Scientific Instruments.)

pressures. The diamond window is by far the most valuable for high pressure studies. It is the hardest material known and is transmissive throughout most of the electromagnetic regions. Generally, two types of diamonds are used — type I and type II. However, there may be variations from diamond to diamond, as has been indicated [53,72,75]. Type I shows absorption at ca. 3, ca. 4—5.5, ca. 7—10 $\mu$m while type II absorbs at ca. 3 and ca. 4—5.5 $\mu$m. Sapphires may be used in the IR region from 2—5 $\mu$m, although pressures are limited to about 12 kbar. Sapphire is promising for Raman pressure studies, since it may be used from $\Delta\nu$ of 500—2000 $cm^{-1}$, before fluorescence becomes a problem. However, pressure limits are low with sapphire windows.

Other measurements have been made with pressure, but these are beyond the scope of this review. For example, electrical conductivities [55,90,91], magnetic susceptibilities [92—100], the Mössbauer effect [101—104], magnetic resonance [105—113], nuclear quadrupole resonance [114—117], X-ray [118—124], and viscosity [125] have all been studied under pressure. However not all these studies have been made with the DAC.

## C. PRESSURE CALIBRATION

It has been mentioned that a pressure gradient exists in the DAC. Duecker and Lippincott [58] have demonstrated that the pressure gradient face is parabolic, with pressures in the center reaching 1—1/2 times those on the edges. Any pressure in the contact area of the diamond is in reality only an average pressure, unless a gasket and a pressure-transmitting fluid is used.

Calibration of the DAC and for that matter other anvil-type cells can be made by several methods. Unfortunately, a number of these methods involve internal calibration incorporating a foreign substance, and the problem of a matrix effect is omnipresent. The methods are listed as follows: (1) The compression of the spring is measured by a Dillon force gauge. The contact area of the diamond is determined by means of microphotographs. One can thus obtain force per unit area of pressure. (2) Solids which undergo phase transitions at known pressure may be used to calibrate the cells. For example, KBr shows a phase transition at 18 kbar; KCl at 20 kbar; $NaNO_2$ at 14 kbar; $HgI_2$ at 13 kbar. These phase transformations can be followed with pressure using a microscope as well as being followed spectroscopically. (3) Calibration may be made by following the change in nickel dimethylglyoxime (NDMG) in the visible absorption region [58,126]. These changes have been related to pressures by the National Bureau of Standards. However, NDMG tends to lose intensity with pressure and the band being monitored is eventually too weak to follow. Other nickel complexes have been suggested [127,128]. (4) Scientists at the National Bureau of Standards [54,55,129—131] suggested calibration of the DAC by following the $R_1R_2$ doublet fluorescence lines at 694.2 and 692.8 nm with a pressure increase. Figure 8 shows the pressure calibration of the ruby $R_1$ fluorescence line. The freezing points of several liquids (e.g., $CCl_4$, $H_2O$, n-$C_7H_{16}$, and $C_2H_5Br$) and two solids, which have character-

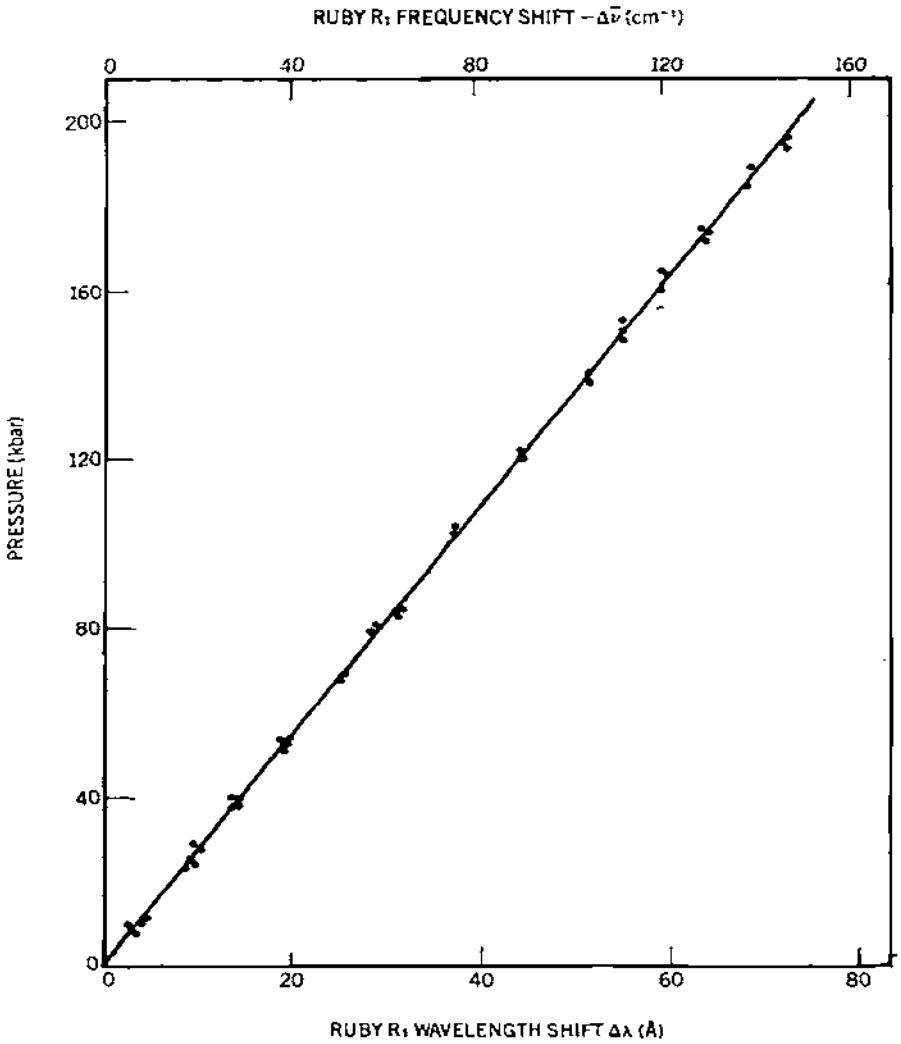


Fig. 8. Pressure calibration of ruby $R_1$ fluorescence line to ca. 160 kbar [55,129—131]. (Figure reproduced through the courtesy of the authors and the American Institute of Physics, New York.)

ized pressure transitions, were used in establishing the pressure response with $cm^{-1}$. It was suggested that the method can be used to high pressures (mbar region) since no significant departure from linearity in the curve occurs, and further that the method is useful to ca. 973 K.

The use of the ruby $R_1$ fluorescence line as a function of pressure has now been extended into the megabar region [90,132—135]. This was done by simultaneously measuring the specific volume of Cu, Mo, Ag and Pb, and

referring the results to isothermal equations of state derived from shock-wave experiments.

The piston-cylinder type cells have been calibrated by measuring bismuth and barium transition pressures or the resistance changes with pressure of various metals (e.g., manganese, lead, iron, barium, calcium and rubidium) [33]. In some cases, pressure transducers are used to measure the pressures [136]. Alternatively, the NDMG or ruby methods, crystals showing phase changes, or a change in the index of refraction may be used. For reviews on pressure calibration see refs. 17 and 137.

## D. CHOICE OF OPTICAL REGIONS TO USE AS A PROBE

The optical region one chooses for pressure studies depends on the particular application. For ionic or pseudo-ionic crystals the far IR region (FIR) is the most useful, since all of the lattice modes occur in this region. For organic compounds the "fingerprint" (mid-IR) region is the most useful. For coordination compounds of the $MX_n$ type, where X = halogen, pseudo-halogen or inorganic anion, the low frequency region is useful as the metal—X vibrations are located there. However, the visible region should be examined conjunctively to monitor the "*d*—*d*" transitions. For coordination compounds involving organic ligands (of the type $ML_nX_m$ where L = organic ligand) the FIR may offer some complications since the organic ligands' strong absorptions could mask the M—X or M—L vibrations. In that case, the visible region may be used. If L = CO or en, one can resort to the mid-IR region using sapphire windows ($\nu_{CO}$ in 5 $\mu$m range), since diamond has absorption in this region. If L = NO one may use the mid-IR region likewise, but in this case one must use diamond windows ($\nu_{NO}$ in the range 6—6.5 $\mu$m), since sapphire shows absorption in this region. For heavy element complexes such as the actinide or lanthanide complexes, the FIR is perhaps the most useful, as "*f*—*f*" transitions appear to be less pressure-sensitive than "*d*—*d*" transitions [138]. Whenever possible, it would be better to use several optical probes to study a particular pressure change.

## E. VIBRATIONAL STUDIES AT HIGH PRESSURES

The opportunity to subject a molecule to an external perturbation such as pressure and measure the resultant changes by spectroscopic techniques, affords the scientist an additional mechanism whereby he can study physical and/or chemical changes. Vibrational spectroscopy becomes a viable method of studying these changes, for in most cases the space group is changed and this is reflected by changes in the vibrational selection rules.

The area of vibrational spectroscopy of molecules subjected to pressure was long neglected [139]. The reasons for the neglect were probably experimental since it was easier to cool or heat a material, and these non-ambient temperature experiments did not require microtechniques in IR or Raman that are

required with pressure measurements. The strides that the matrix isolation technique has made in the past 10 years attests to this. However, the advent of the DAC in 1959 [48] generated the notion that vibrational spectroscopic techniques used conjunctively with pressure were possible. This paper is planned to present a review of the accomplishments of the past 20 or so years, since Weir and co-workers constructed the DAC [48]. In most cases the review will concern itself with results obtained with the DAC.

*(i) Inorganic compounds*

Primary motivations in studying solid inorganic systems have been based on studying pressure effects on various polymorphs, those stable under ambient conditions and those achieved only under high pressures. In this way phase diagrams, previously unknown, can be constructed or adjusted. In cases where no X-ray is known (e.g., phases obtainable only at elevated conditions of temperature and pressure) some inference may be obtained on the nature of the space group involved from the spectroscopic results. In certain instances interest has been based on obtaining order-disorder information existing in the various phases of a material (for example, electrical conducting phases). Comparisons of intra- and intermolecular forces, the latter being pressure sensitive, are also of interest. Of interest are hydrogen bonded systems where pressure shows effects which can be observed by studying the vibrational spectra.

*(1) Mercuric halides*

Adams and Appleby [140] have investigated the halides of Hg(II) under high pressure. The three phases (I, II and IV), of $HgCl_2$ have been subjected to pressures up to 30 kbar. Results are shown in Table 8. The Raman and IR spectra of phases I and IV were found to be similar, and it was concluded that a second-order transition characterized by molecular orientation with retention of the space group was involved. Phase II was found to be entirely different and to approximate a $T_h^6$ structure with $z = 4$, based on the spectroscopic results. Phases I and IV possess a $D_{2h}^{16}$ space group with $z = 4$.

All four phases of $HgBr_2$ (I, II, III and IV) were investigated by Raman and IR techniques to 50 kbar [141]. Phases I and II were considered to have similar structures. Phase III appears to possess a $C_{2h}$ space group, and phase IV probably has a $CdI_2$ structure. These conclusions were reached, based on the spectroscopic results obtained. Table 9 tabulates the Raman frequencies at various pressures.

Early superficial Raman experiments with $HgI_2$ have been made [59,60]. In a more thorough study the high temperature (127°C) phase and the high pressure phase (ca. 13 kbar) of $HgI_2$ were compared, using Raman and far IR data [142]. The red, ambient temperature, $HgI_2$ has a $P4_2/nmc$ ($D_{4h}^{15}$) space group, $z = 2$, with 4 iodine atoms around the mercury atom [143]. At 127°C it turns yellow and this phase has a $Cmc2_1$ space group with $z = 4$ [144]. At

TABLE 8

Raman and IR results for phases I, IV and II in the $HgCl_2$ system [140]

| Phase | Raman ($cm^{-1}$) | IR ($cm^{-1}$) |
|---|---|---|
| I (Ambient pressure) | 383 (vvw) | 370 (vs) |
| | 315 (s, sp) | 330 (vw) |
| | 167 (vvw) | 310 (w) |
| | 126 (w) | 100 (vs) |
| | 74 (m) | 75 (sh) |
| | 43 (vw) | |
| | 23 (m) | |
| | 18 (s) | |
| IV (8.5 kbar) | 386 (vvw) | 370 (vs) |
| | 316 (s, sp) | 330 (w) |
| | 170 (vvw) | 310 (w) |
| | 144 (w) | 100 (vs) |
| | 133 (w) | 77 (sh) |
| | 77 (m) | |
| | 51 (w, sh) | |
| | 41 (vvw) | |
| | 21 (m) | |
| II (30 kbar) | 312 (vs) | 369 (vs) |
| | 178 (s) | 100 (vs) |
| | | 72 (vs) |

13 kbar red $HgI_2$ converts to a yellow phase. Differences are observed in both the IR and Raman spectra of the two yellow phases. The high pressure phase has a more complex far IR spectrum than the high temperature phase, especially in the 80 $cm^{-1}$ region. In the Raman spectrum the 145 $cm^{-1}$ band in the high pressure phase has a shoulder, which is missing in the low temperature

TABLE 9

Raman frequencies ($cm^{-1}$) for $HgBr_2$ at various pressures (R.T.) [141]

| | Pressure (kbar) | | | | | | |
|---|---|---|---|---|---|---|---|
| | 0 | 6.3 | 18.8 | 23.3 | 31.6 | 35.7 | 49.5 |
| Phase | I | II | II | III | III | IV | IV |
| | | | | 191 | 191 | | |
| | 186 | 185 | 184 | 184 | 184 | 179 | 176 |
| | | | | 74 | 77 | 78.5 | 77 |
| | 57 | 61 | 60 | 60 | 69 | | |
| | | | | 50 | 49 | | |
| | 40 | 38 | | | | | |
| | 17.5 | 22 | 24 | | | | |
| | 15 | 17 | 18 | | | | |

phase. The low temperature phase has Raman bands at 15 and 11.5 $cm^{-1}$, which are missing in the pressure phase. Although the high pressure phase of $HgI_2$ remains unknown, the vibrational spectrum resembles that of phase III of $HgBr_2$, and would thus appear to have a structure with a higher coordination number, consistent with consequences of increased pressure.

Studies of the effect of pressure on the $\nu_{HgCl}$ vibration in $HgCl_2 \cdot$ dioxane have been made [145]. This vibration shifts 18 $cm^{-1}$ towards lower energy, while modes of the organic ligand bands at 854, 614 and 290 $cm^{-1}$ are raised by ca. 5 $cm^{-1}$.

*(2) Alkali metal cyanides*

The various polymorphic phases of KCN and NaCN have been investigated using vibrational spectroscopy at high pressures [146]. Table 10 lists structural data for the polymorphs of KCN and NaCN. Raman frequencies are listed in Table 11 for KCN polymorphs at various pressures. The behavior of the cyanide vibration with pressure in KCN and NaCN is shown in Table 12. The Raman scattering of $K[Ag(CN)_2]$ has recently been measured to 18 kbar [146a]. Two high-pressure polymorphs were identified. A dramatic change in the pressure dependency of the CN stretching vibration was noted. The pressure of other internal and external modes was also determined.

*(3) Nitrates, carbonates*

Infrared spectra of $KNO_3$ have been obtained at pressures up to 40 kbar [147]. The pressure range of $KNO_3$ (III) with a symmetry $R3m$ ($C_{3v}^5$) with $z = 1$, is very narrow and at 4 kbar and 38°C converts to $KNO_3$ (IV). For this phase a new band was observed at 717 $cm^{-1}$. The 825 $cm^{-1}$ absorption shifts to 831 $cm^{-1}$ and increases in intensity with pressure. $\nu_3$ and $\nu_1$ show a small shift to higher frequency, and a slight increase in intensity. The various combinations involving the $NO_3^-$ vibration lose intensity with pressure. It was observed that $\nu_1$ is more sensitive to pressure than $\nu_4$, and $\nu_2$ is insensitive. The

TABLE 10

Structural data for the NaCN and KCN polymorphs [146]

| Phase | | Structure | $Z$ |
|---|---|---|---|
| KCN | I | Cubic, $F_{m3m}(O_h^5)$ | 4 |
| | III | Cubic, $P_{m3m}(O_h^1)$ | 1 |
| | IV | Monoclinic, $Cm(C_s^3)$ | 2 |
| | V | Orthorhombic, $I_{mmm}(D_{2h}^{25})$ | 2 |
| | VI | Orthorhombic, $P_{mmn}(D_{2h}^{13})$ | 2 |
| NaCN | I | Isostructural with KCN I | |
| | II | Isostructural with KCN V | |
| | III | Isostructural with KCN VI | |

TABLE 11

Raman frequencies ($cm^{-1}$) for KCN polymorphs [146]

| Pressure (kbar) | 0.001 | 6.58 | 16.5 | 20.1 | 27.6 | 0.001 | 0.001 | 21.7 |
|---|---|---|---|---|---|---|---|---|
| Temp. (K) | 293 | | | | | 87 | 60 | 383 |
| Phase | I | I | I | I & IV | IV | V | VI | III |
| $\nu_{CN}$ | 2078.2 [a] | 2083.5 | 2090 | 2090<br>2088 (sh) | 2090 | 2080.0 [a] | 2081.1 [a] | 2090 |

[a] ± 0.2 $cm^{-1}$; all others ± 0.5 $cm^{-1}$

TABLE 12

| $\nu_{CN}$ | $d\nu/dp$ ($cm^{-1}$ $kbar^{-1}$) [146] |
|---|---|
| KCN I | 0.50 (20°C) |
| KCN I | 0.57-1 (110 C) |
| KCN III | 0.45 (110°C) |
| KCN IV | 0.32 (20° C) |
| NaCN II | 0.57 |

results are consistent with a unit cell of high occupancy and low symmetry.

$AgNO_3$ has also been investigated at high pressure [148]. Adams and Sharma [148] have studied phases I, II, III and metastable phase V. In the latter phase doublets occur in $\nu_3$, $\nu_1$ and $(\nu_1 + \nu_4)$ regions, and with the shape of the $\nu_3$ envelope are all indicative of a low site symmetry and relatively high unit cell occupancy.

The first solid studied in the DAC was calcite, $CaCO_3$ [149]. The results showed that $\nu_1$, normally IR inactive, appeared in the spectrum with pressure; $\nu_2$ shifted from 882 to 865 $cm^{-1}$ and splitting of $\nu_4$ occurred. Other studies were made with calcite up to 61 kbar. The authors pointed out that the spectra at higher pressures resembled that of a calcium carbonate polymorph, vaterite, with a hexagonal unit cell containing 2 or more molecules per unit cell. Fong and Nicol [150] have studied $CaCO_3$ to 40 kbar, and have interpreted their data in terms of two phases of calcite, II and III, occurring at 14 kbar and 18 kbar. Recent Raman spectra have verified that the high pressure phases are not aragonite [151]. Only superficial studies have been made with aragonite and $MgCO_3$ under pressure [48].

*(4) $NaNO_2$ and $KNO_2$*

Infrared spectra of $KNO_2$ and $NaNO_2$ and Raman spectra of the polymorphs of $KNO_2$ have been studied at high pressures [152,153]. $NaNO_2$ ($C_{2v}^{20}$, $z = 1$) undergoes a phase transition at 39°C and 10 kbar and $KNO_2$ undergoes a transition at 6.3 kbar. In the IR studies it was determined that the symmetric modes lose intensity with pressure and all bands undergo blue shifts. The Raman studies have led to conclusions concerning the nature of the polymorphs and the order-disorder in these phases.

*(5) Dihydrogen phosphates*

The paraelectric crystals of $KH_2PO_4$ and $RbH_2PO_4$ were studied by IR at pressures to 60 kbar [154]. For both compounds the protons were found to be dynamically disordered between the two possible O·H···O sites connecting the $PO_4^{3-}$ groups. A new phase was found at 10 kbar in which the hydrogens became ordered while the $PO_4^{3-}$ tetrahedra became disordered. In pressure

studies of $KH_2PO_4$ to 9.3 kbar a soft mode in the crystal became underdamped with the application of pressure [155]. Studies with $RbH_2PO_4$ were made at 21 kbar using Raman spectra as the optical probe [156]. These results indicated a large decrease in transition temperature with pressure and a disappearance of the ferroelectric state at all temperatures for $p \geqslant 15.2$ kbar, and a decrease with pressure of the Curie constant and dielectric constant in the paraelectric phase.

*(6) Molybdates, tungstates, sulfates*

The Raman spectra of $CaMoO_4$ and $CaWO_4$ have been obtained at pressures to 40 kbar [157]. A new pressure phase for each compound was found. The pressure dependencies of the internal modes for these compounds were determined and found to range from 0.0 to 1.0 $cm^{-1}$ $kbar^{-1}$.

Some sulfates were superficially examined at high pressures [64]. $\nu_4$ of $SO_4^{2-}$ anion showed shifts of 3 $cm^{-1}$ at 35 kbar, while a lattice mode at 183 $cm^{-1}$ showed a blue shift of 52 $cm^{-1}$.

*(7) Bihalide salts*

The bihalide salts of $NaHF_2$, $KHF_2$, $NH_4HF_2$, $(CH_3)_4NHCl_2$ and $(C_2H_5)_4NHCl_2$ were investigated by IR techniques at pressures up to 40 kbar [158]. In these strong hydrogen bonded systems the $\nu_3$ vibration in the $HX_2^-$ anion shifts to higher frequencies while the $\nu_2$ vibration shifts to lower energies with an increase in pressure. The $\nu_1$ frequency was deduced from the behavior of combination bands and found to shift toward higher frequencies. These results are typical expectations for a simple model of strong hydrogen bonding. A new phase of $NaHF_2$ was found at 40 kbar.

*(8) Ionic conductors*

The pressure dependent Raman spectra of the fast ion conductors $\beta$-$Ag_2HgI_4$ and $\beta$-$Cu_2HgI_4$ were measured [159]. The Raman spectra of $\beta$-$Cu_2HgI_4$ ($I42m$ ($D_{2d}^{11}$), $z = 2$) was followed at 25°C to 24 kbar, and no phase transition was observed. The breathing motion of the iodide lattice against the $Cu^{2+}$ ions at 85 $cm^{-1}$ undergoes a more rapid blue shift than the Hg—I stretch at 127 $cm^{-1}$, indicative of greater anharmonicity in the $CuI_4$ stretching mode as compared to the $HgI_4$ stretch. The 36 $cm^{-1}$ mode shows a negative pressure dependence.

$\beta$-$Ag_2HgI_4$ ($I\bar{4}$ ($S_4^2$), $z = 2$) shows several phase changes in the 0—10 kbar region. Table 13 shows band positions in $Ag_2HgI_4$ at various pressures and at 60°C. At 6.1 kbar and 25°C, the HgI stretching vibration lowers from 124 to 116 $cm^{-1}$ and may indicate a change from 4-coordinate to a 6-coordinate environment. Figure 9 shows the Raman spectra of $\beta$-$Ag_2HgI_4$ as a function of pressure. A second phase is observed between 7.5—44 kbar and another phase at pressures greater than 44 kbar.

The Raman spectra of these materials have been found useful in screening potential ionic conductors [160,161]. Broad Raman bands are indicative of

TABLE 13

Band positions of polycrystalline $Ag_2HgI_4$ at various pressures[a] [159]

| Temp. (°C) | Pressure (kbar) | Position ($cm^{-1}$) | | | | | | | |
|---|---|---|---|---|---|---|---|---|---|
| 25 | 0 | | 24.2 (s) | 29.5 (w) | | 34.9 (s) | 80 (w, br) | 106 (w, br) | 122.1 (s) |
| 24 | 4 | | 23.8 | — | | 35.1 | — | — | 124.0 |
| 25 | 6 | 19.1 (s) | | | 32.8 (w) | | | 115.7(m) | |
| 25 | 8 | 19.3 | | | 34.2 | | | 115.9 | |
| 60 | 0 | 17 (s, br) | | | 123 (s, br) | | ~142 (m, sh) | | |
| 60 | 6 | | 29 (m) | 114 (vs) | | | | | |

[a] A gasketed diamond anvil cell with paraffin oil as a pressure transmitting liquid was used.

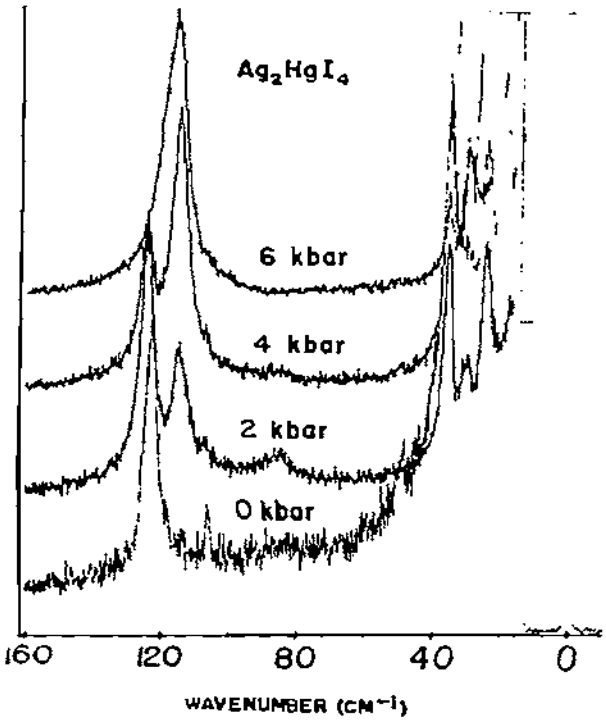


Fig. 9. Raman spectra of $\beta$-$Ag_2HgI_4$ as a function of pressure [159]. (Figure reproduced through the courtesy of the authors and the American Institute of Physics, New York.)

ionic conductors and disorder. The sudden sharpening of the bands at 6.1 kbar is an indication of electronic conduction and a more highly ordered structure. The results are used to determine the anharmonicity in superionic conductors [159]. Both CuI and HgI modes are highly anharmonic, and a highly anharmonic potential may be important in providing a low energy barrier for ion motion and ionic conductivity.

*(9) Miscellaneous inorganic compounds*

*(a) Ammonium halides.* Wong and Whalley [162] have made a Raman study of $NH_4F$ and Ebisuzaki and Nicol [163] have examined $NH_4Cl$ under pressure using Raman spectroscopy. At 10 kbar a disordered-ordered phase transition takes place in $NH_4Cl$. The lattice mode involving movement of the $NH_4^+$ and $Cl^-$ sublattices shows a pressure dependency of 2.65 $cm^{-1}$ $kbar^{-1}$ in the disordered (low pressure) phase. The librational mode behaves similarly. With the exception of the $\nu_2$ bending vibration in $NH_4^+$ the internal modes all show negative pressure dependencies varying from $-0.1$ to $-1.2$ $cm^{-1}$ $kbar^{-1}$ and are attributed to the increased hydrogen bonding occurring in the ordered high pressure phase.

*(b) Solid nitrogen.* The Raman spectra of the three known phases of solid nitrogen at high pressures (0—10 kbar) and low temperature (8—220 K) were obtained [164]. The high pressure $\gamma$ phase is tetragonal with $D_{4h}^{14}$ space group and $z = 2$. The observed frequencies and relative integrated intensities were determined. Table 14 tabulates results at various temperatures. By comparing the results with calculated frequencies and relative intensities the low- and high-frequency bands in the lattice region were assigned as librational modes, $E_g$ and $B_{1g}$, respectively.

*(c) Water ice.* In passing I wish to cite the work of Whalley and co-workers on water ices. The IR spectra of water ice II, III, V, VI and VII at appropriate pressures and temperatures were measured [165]. The Raman spectra for ices $I_h$, $I_c$, II, III and V were also obtained by Marckmann and Whalley [166].

*(ii) Ionic and pseudo ionic crystals with lattice vibrations*

Considerable interest has developed in examining the pressure dependence of vibrational lattice modes in neat, ionic and pseudo ionic, and mixed crystals. The interest in pressure studies stems from results which can be obtained that can be used for testing lattice dynamics theory. Results are generally reported in terms of a Grüneisen parameter. Both temperature and pressure data provide information on anharmonic contributions to the lattice frequency shift. The temperature dependence of the peak position and half-width of lattice modes consist of the purely volume dependent part of the Grüneisen equation of state and the anharmonic contributions. On the other hand, the pressure dependence of peak position arises chiefly from the volume dependent part of the Grüneisen equation. Comparison of the Grüneisen parameter obtained from both methods can provide some estimate of anharmonicity existing in these solids.

TABLE 14

Observed Raman frequencies and relative intensities for the $\gamma$-phase of solid $N_2$ [164]

| Temp. (K) | $\nu$(cm$^{-1}$) | Relative integrated intensity |
|---|---|---|
| 35 | 57.5 | 2 |
| | 95.5 | 4.5 |
| | 2329 | 1 |
| 20 | 58.2 | 5.5 |
| | 102.5 | 3 |
| | 2330 | 1 |
| 8 | 58.4 | 7 |
| | 103.6 | 2.5 |
| | 2331 | 1 |

Tables 15—19 list some ionic lattice frequencies [167]. Most of the frequencies for the transverse optical lattice modes ($\nu_{TO}$) in ionic salts are found below 300 $cm^{-1}$. The capability of measuring vibrational spectra in the far-IR region under pressure allowed study of these vibrations for the first time in this manner. The longitudinal mode ($\nu_{LO}$) is more difficult to study in the IR. It is not normally observed at 90° incident radiation. Berreman [168] observed the longitudinal mode for a thin film of LiF with an oblique incident radiation, and longitudinal optical modes of the silver halides have been studied by a similar technique [171]. The longitudinal modes can be observed with a diamond cell and highly converging oblique radiation arriving from the beam condenser. They appear as shoulders on the main, intense transverse vibrational bands, and are not easily studied with pressure in the IR, for they are less pressure sensitive than the transverse modes and, because of the high-frequency shift of the $\nu_{TO}$ band, become lost in the $\nu_{TO}$ envelope. In more covalent solids $\nu_{TO}$ approaches $\nu_{LO}$, and in a homopolar covalent crystal, $\nu_{TO}$ may equal $\nu_{LO}$. In this instance, a very broad absorption is observed, which shows very little frequency shift with pressure.

Figure 10 shows a comparison of several $\nu_{TO}$ frequencies with pressure. The $\nu_{LO}$ pressure dependence for NaF is shown in Fig. 11. In this system the separation between $\nu_{LO}$ and $\nu_{TO}$ is sufficiently large to make possible a determination of the pressure dependence of both optical modes.

In general, ionic lattice vibrations shift toward higher frequencies with increasing pressure, although red shifts can be observed. The shifts at pressures of up to 50 kbar may be considerable; however, not all ionic lattice vibrations show dramatic shifts, since the compressibility of the solid is involved. The relationship between the change in frequency with pressure for simple cubic ionic solids, where the three crystallographic axes are equal, is given in eqn. (1)

$$\gamma\chi\nu = (\partial\nu/\partial p)_T \qquad (1)$$

where $\gamma$ is the Grüneisen parameter, $\chi$ is the isothermal compressibility of the

TABLE 15

Lattice vibrations for alkali halides[a]

| Halide | $\nu_{TO}$ ($cm^{-1}$) | Halide | $\nu_{TO}$ ($cm^{-1}$) | Halide | $\nu_{TO}$ ($cm^{-1}$) |
|---|---|---|---|---|---|
| LiF | 307 | NaI | 117 | RbCl | 118 |
| LiCl | 191 | KF | 190 | RbBr | 88 |
| LiBr | 159 | KCl | 141 | RbI | 77 |
| NaF | 246 | KBr | 113 | CsCl[b] | 99 |
| NaCl | 164 | KI | 98 | CsBr[b] | 74 |
| NaBr | 134 | RbF | 156 | CsI[b] | 62 |

[a] Ref. 169. [b] Ref. 170.

TABLE 16

Lattice vibrations for several other ionic cystals[a]

| | $\nu_{TO}$ ($cm^{-1}$) | $\nu_{LO}$ ($cm^{-1}$) |
|---|---|---|
| TlCl | 63 | 158 |
| TlBr | 43 | 101 |
| AgCl | 106 | 196 |
| AgBr | 79 | 138 |
| MgO | 401 | 718 |
| NiO | 401 | 580 |
| CoO | 349 | 546 |
| MnO | 262 | 552 |

[a] IR data from S.S. Mitra, AFCRL-69-0468, Air Force Cambridge Research Labs., Oct. 1969.

TABLE 17

Lattice vibrations for II—VI compounds[a]

| | $\nu_{TO}$ ($cm^{-1}$) | $\nu_{LO}$ ($cm^{-1}$) |
|---|---|---|
| ZnO | (∥) 377 | 575 |
| | (⊥) 406 | 589 |
| ZnS | 278 | 350 |
| ZnSe | 205 | 253 |
| ZnTe | 179 | 206 |
| CdS | 239 | 306 |
| CdSe | 170 | 211 |
| CdTe | 125 | 151 |

[a] IR data from S.S. Mitra, AFCRL-69-0468, Air Force Cambridge Research Labs., Oct. 1969.

TABLE 18

Lattice vibrations for III—V compounds[a]

| | $\nu_{TO}$ ($cm^{-1}$) | $\nu_{LO}$ ($cm^{-1}$) |
|---|---|---|
| InSb | 185 | 197 |
| InAs | 219 | 243 |
| InP | 304 | 345 |
| GaSb | 231 | 240 |
| GaAs | 269 | 292 |
| GaP | 367 | 403 |
| AlSb | 319 | 340 |
| AlP | 440 | 501 |
| AlN | 667 | 916 |
| BP | 820 | 834 |
| BN | 1056 | 1304 |

[a] From S.S. Mitra, AFCRL-69-0468, Air Force Cambridge Research Labs., Oct. 1969.

TABLE 19

Lattice vibrations for IV—IV compounds [a]

| | $\nu_{TO}$ ($cm^{-1}$) | $\nu_{LO}$ ($cm^{-1}$) |
|---|---|---|
| Diamond | 1332 [b] | 1332 [b] |
| Silicon | 520 [b] | 520 [b] |
| Germanium | 301 [b] | 301 [b] |
| SiC | 793 [c] | 970 [c] |

[a] From S.S. Mitra, AFCRL-69-0468, Air Force Cambridge Research Labs., Oct. 1969.
[b] Raman frequencies. [c] IR frequencies.

solid, and $\nu$ is the frequency of the lattice mode. For non-compressible solids, it is possible that only small shifts will occur. For example, the lattice modes of zirconium and hafnium oxides failed to show significant shifts at 40 kbar [67]. It is also possible that the pressure effects may be different in noncubic crystals having different axes parameters, depending on which axis becomes compressible [172,173].

The data obtained from studies of the pressure dependence of the $\kappa \simeq 0$

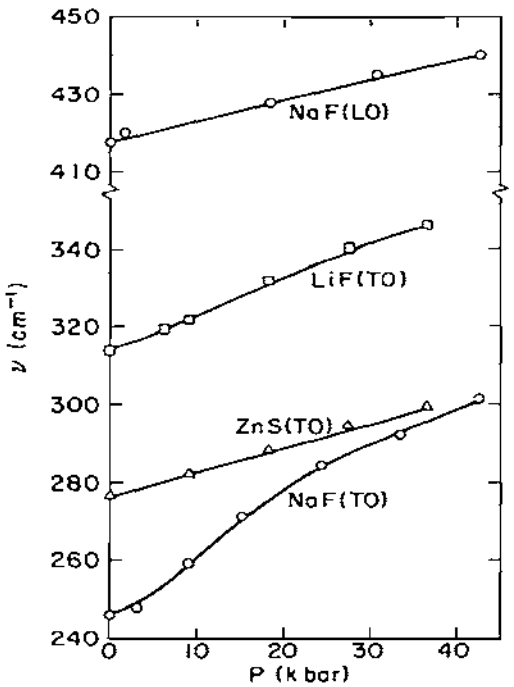


Fig. 10. Pressure dependencies of several lattice vibrations [139]. (Figure reproduced through the courtesy of the authors and Academic Press, New York.)

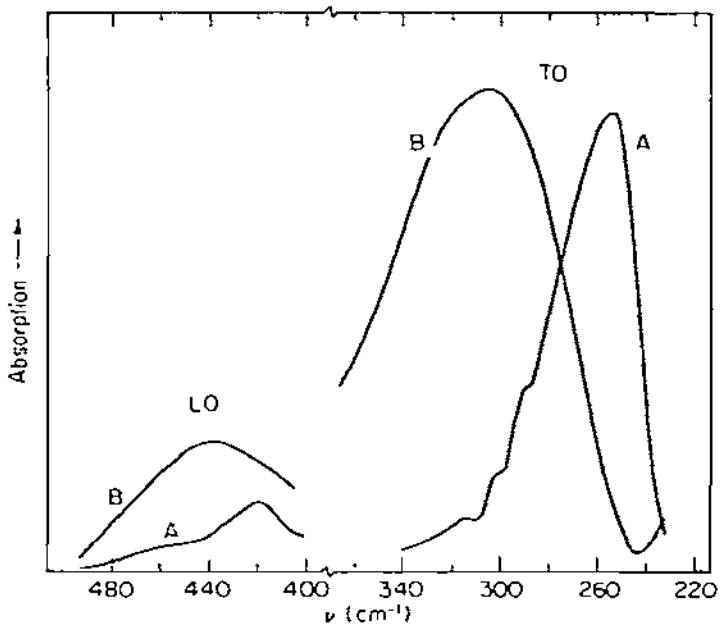


Fig. 11. Comparison of TO and LO modes in NaF with and without pressure [139]. (Figure reproduced through the courtesy of the authors and Academic Press, New York.)

lattice vibrations of ionic crystals [174], when combined with data from studies of these modes with temperature [175], may allow calculation of the anharmonic interactions taking place, and contribute to a better understanding of the lattice dynamics of these solids. It is possible to distinguish between the purely volume-dependent contribution and the contribution from various anharmonic terms in the crystal Hamiltonian [176]. Fig. 12 shows a plot of $\ln \nu/\nu_0$ vs. $\ln V/V_0$ for several optical modes. The data have been obtained from pressure and high-temperature studies [174—176], $P$-$V$ data from Pagannone and and Drickamer [177], and from Cline and Stephens [178]. It can be observed that the straight line extrapolated from the pressure domain does not coincide with the line obtained from the temperature data. The difference may be attributed to the anharmonic contribution to the frequency shift (known as the self-energy shift), which increases steadily with increasing temperature of LiF. A similar analysis was made for KBr and in this crystal the self-energy shift is negligible. Results obtained for RbI using other techniques [175,179] also indicated negligible self-energy shifts.

The results obtained for the Grüneisen parameters for the long-wavelength optical modes from eqns. (1) and (2)

$$\lambda_{j(k)} = -\partial \ln \nu_j(k)/\partial \ln V \qquad (2)$$

are given in Table 20. The agreement with the calculations made from those

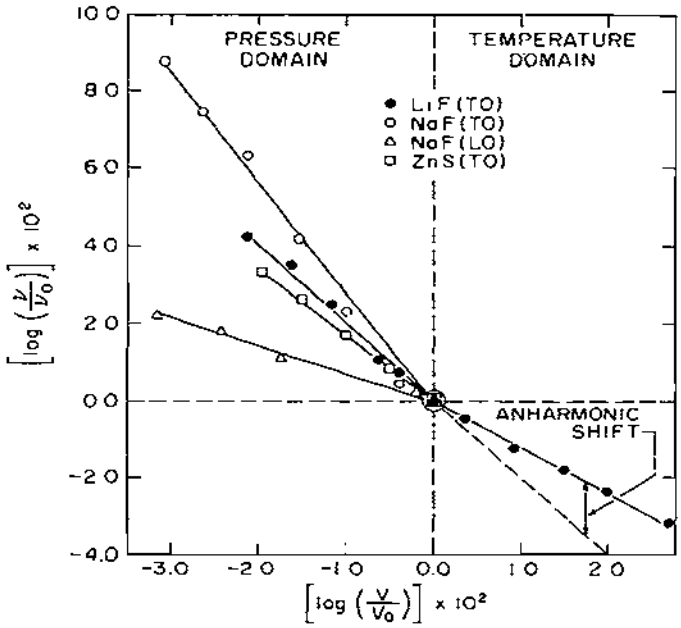


Fig. 12. Plot of $\ln \nu/\nu_0$ vs. $\ln V/V_0$ for several optic modes [139]. (Figure reproduced through the courtesy of the authors and Academic Press, New York.)

assuming a rigid-ion model with central forces incorporating repulsion terms of the Born-Mayer [$\exp(-r/p)$] and inverse-power ($r^{-n}$) type is good. The results using Cowley's theory give somewhat larger values of $\gamma$.

The pressure dependencies of two phases of a solid can be determined by these techniques. Such studies have been made with KBr and KCl [176]. Figure 13 shows the TO mode of KCl as a function of pressure and illustrates the difficulty of studying phase transitions. The pressure gradient across the

TABLE 20

Grüneisen parameters for the long-wavelength optical modes

| | Experimental | | Calculated | | | | |
|---|---|---|---|---|---|---|---|
| | Eqn. (1) | Eqn. (2) | Born–Mayer [a] | $r^{-n}$ repulsion [b] | Cowley [c] | Model I [d] | Model II [d] |
| LiF | 2.15 | 2.59 | 2.44 | 3.46 | | | |
| NaF | 2.80 | 2.95 | 2.43 | 3.00 | | | |
| KBr | | 2.83 | 2.52 | 2.95 | 3.27 | ~3.0 | ~2.6 |
| KCl | | 2.46 | 2.52 | 2.92 | | | |

[a] Ref. 180. [b] Ref. 181. [c] Ref. 182. [d] Ref. 183.

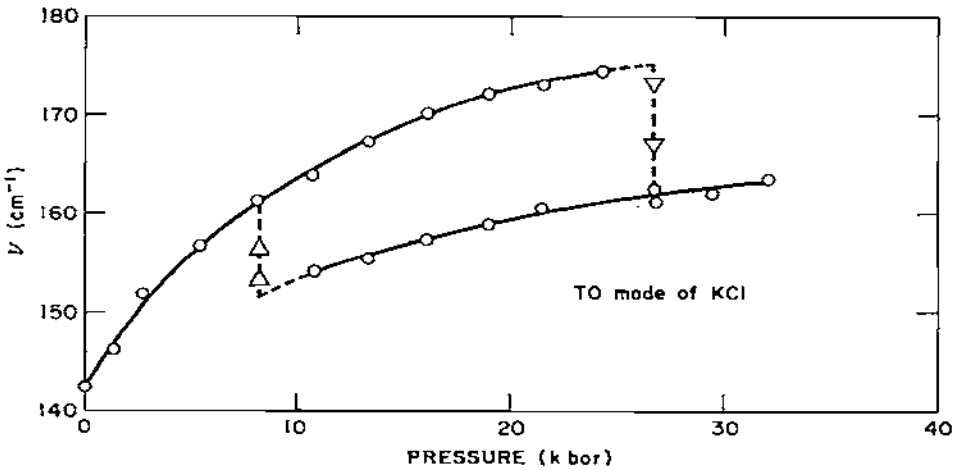


Fig. 13. TO mode of KCl as a function of pressure [139]. (Figure reproduced through the courtesy of the authors and Academic Press, New York.)

diamond anvils prevents the detection of a sharp transition pressure and both phases appear over a range of pressures. The high-pressure phase (CsCl structure) appears at 16 kbar for KBr and at 24 kbar for KCl. The conversion to the the high-pressure phase is complete at 26 and 30 kbar for KBr and KCl, respectively. For a limited average pressure range the TO mode of both the low- and high-pressure phases can be detected, with a gradual decrease in the intensity of the low-pressure phase and an increase in that of the high-pressure phase. With the reduction of pressure, the frequencies of the CsCl phase do not coincide with those determined from increasing pressures (maximum experimental error $\pm 2$ cm$^{-1}$). The low-pressure phase does not reappear until 11 and 16 kbar for KBr and KCl, respectively. Some of these discrepancies can be attributed to the sluggishness of the system and friction created within the cell.

The vibrational frequency decreases at the transition pressure by about 10—12%. The ratio of TO frequency of the CsCl phase to that of the TO frequency in the NaCl phase should equal the square root of the coordination number of each phase; e.g., $\frac{3}{8}^{1/2}$ or 0.87. The observed ratio for KBr is 0.88 and that of KCl is 0.92.

It has been found [184] that the $k \simeq 0$ TO frequency of the alkali halides of NaCl structure is proportional to $(a/\chi\mu)^{1/2}$, where $a$ is the lattice constant, $\mu$ is the reduced mass per unit cell, and $\chi$ is the compressibility. The same is true for the CsCl structure, as illustrated in Fig. 14.

Pressure studies of mixed crystals have recently been reported for $CdS_{1-x}Se_x$, $ZnS_{1-x}Se_x$ [185] and $KCl_{1-x}Br_x$ [186]. In both the two-mode system $ZnS_{1-x}Se_x$, and the one-mode system $KCl_{1-x}Br_x$, the pressure dependencies of the various mixtures of the mixed crystals parallel those obtained for the pure components. Figure 15 illustrates the pressure dependence

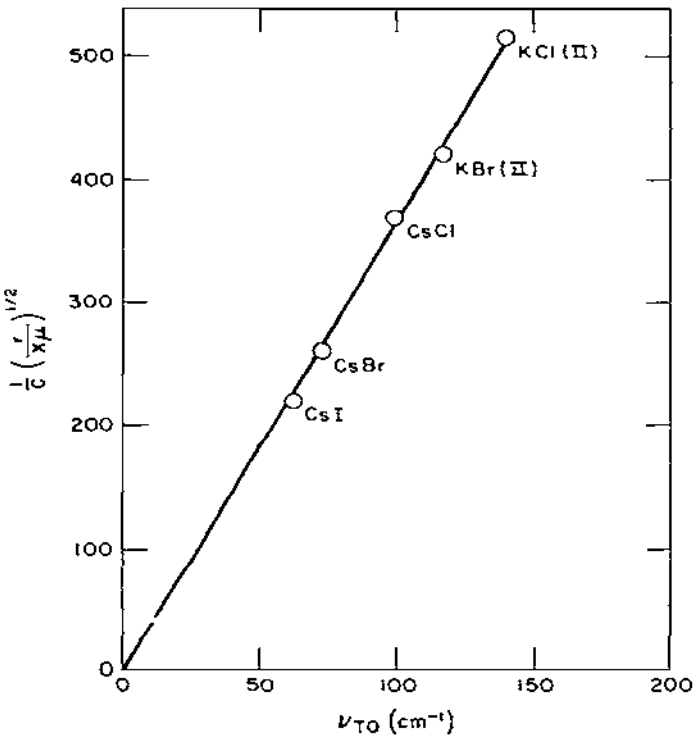


Fig. 14. Plot of TO mode frequency for several CsCl-type salts vs. $1/c(r/x\mu)^{1/2}$ [139]. (Figure reproduced through the courtesy of the authors and Academic Press, New York.)

of the high frequency mode in the $ZnS_{1-x}Se_x$ system.

Certain molecular lattice modes were investigated by McDevitt et al. [67] and Fondere et al. [187]. The experiments are more difficult to perform since a thicker sample is needed, and gaskets are necessary to accomplish this. Molecular lattice vibrations have been observed to also shift toward higher frequencies with increasing pressure. Raman experiments [188] have demonstrated that molecular lattice vibrations are more sensitive to pressure than ionic lattice modes, as expected.

Pressure dependencies of KI, RbI and their mixed crystals have been determined [189]. The mode Grüneisen parameters were determined and compared well with the calculated parameters from a rigid ion model using the Born-Mayer type potentials. Similar measurements have also been made for IR-active phonon modes in alkali-earth fluorides [190]. The pressure dependence of the Raman spectra of the alkaline-earth fluorides is also available [191]. Several anti-fluorite structures have been studied at high pressures (e.g., $Mg_2Si$, $Mg_2Ge$, $Mg_2Sr$) [192].

First and second order Raman spectra have recently been obtained on hexa-

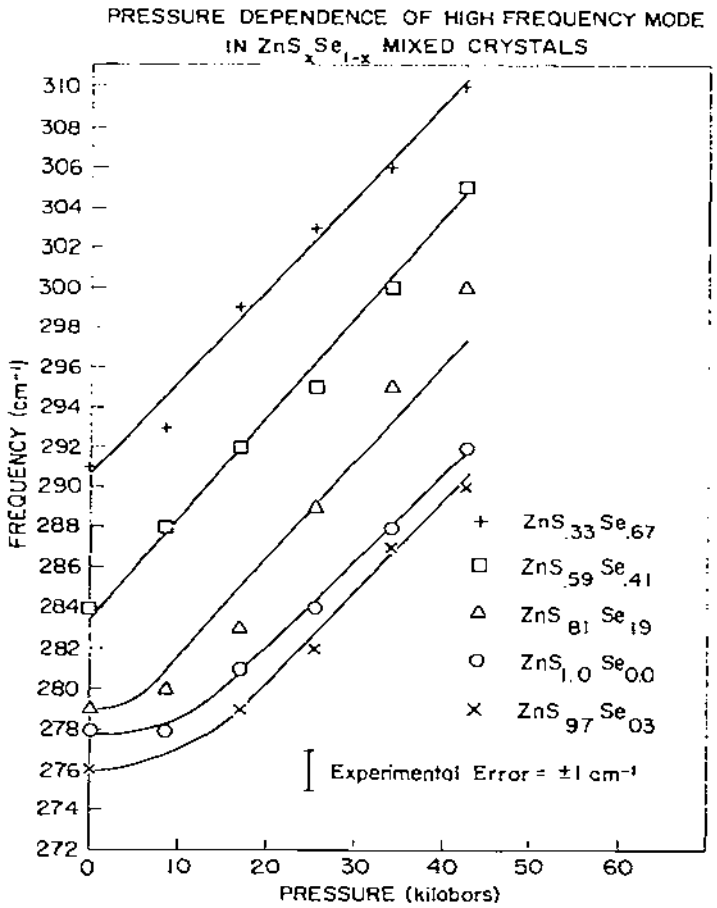


Fig. 15. Pressure dependencies of high frequency mode in $ZnS_{1-x}Se_x$ mixed crystals [185]. (Figure reproduced through the courtesy of the authors and Academic Press, New York.)

gonal ZnS (wurtzite) at pressures to 40 kbar [193]. No phase transformation to a cubic phase was observed. The Grüneisen parameters were found to be 0.99 for the $\nu_{LO}$ mode and 1.81 for the $\nu_{TO}$ mode. For the $\nu_{TA}$ mode the value ranged from —1.79 to 2.38 in the second-order spectrum. The splitting between $\nu_{TO}$ and $\nu_{LO}$ decreases with pressure. Raman (one- and two-phonon) spectra of GaP at pressures to 135 kbar were determined [194]. Mode Grüneisen parameters were calculated. Raman and far-IR studies to 45 kbar of the phase transition in paratellurite ($TeO_2$) were made recently [195]. At the phase transition at 9 kbar an $E$ mode at 122 $cm^{-1}$ splits into two components in the IR and Raman spectra. These results aided in assigning the various phonon modes in $TeO_2$. Raman spectra to 4 kbar were obtained for $TiO_2$

(rutile) [86]. Grüneisen parameters for each lattice mode were obtained. The $B_{1g}$ phonon mode was found to have a negative pressure dependency. These results agree with earlier pressure measurements made to 40 kbar, which demonstrated a $d\nu/dp$ for this mode as $-0.3 \pm 0.1$ cm$^{-1}$ kbar$^{-1}$ [196]. This mode softens as well with decreasing temperature, although only slightly. The unusual pressure dependency for this vibration may have important implications relative to pressure-induced phase transitions in rutile, as well as in other crystals with this structure.

*(iii) Coordination compounds*

Interest in solid coordination compounds has centered on the behavior of various vibrational transitions under high pressures. Considerable interest has also developed in changes occurring with pressure in spin states and in oxidation states, and to identify these changes with far IR spectroscopy. Perhaps of most significance are the structural transformations which pressure has induced. The latter effects have served to test the theoretical predictions of Pearson [197] and Bader [198] regarding stability of various geometrical configurations. It is also possible that these studies provide a foundation for anticipated ultra-high pressure measurements of minerals.

*(1) High pressure effects on vibrational transitions*

As more research involving high pressure effects accumulates with time, it has become clear that certain vibrations are more sensitive to pressure than others. For example, vibrations which involve expansion of molecular volume appear to be more sensitive to pressure. Attempts to quantify the behavior of vibrations with pressure may never be realized for the application of pressure to solids involves many factors, and screening these factors may be an impossible task. Such factors as packing effects, compressibilities, nature of bonds (ionic vs. covalent), crystal field stabilization energy, steric effects, electronic repulsions, electronic delocalization, and other effects all contribute toward pressure-sensitivity of various vibrations in a molecule.

Examples of pressure effects on vibrations in different molecules will be discussed in the following sections.

*(a) Ligand vibration.* Relatively little attention has been paid to the effects of pressure on ligand vibrational modes. In a study of pyrazine and its complexes up to 72 kbar several observations could be made [199]. (1) Ligand bonds showed blue shifts and were less sensitive than the bands of the complexes. (2) Some bands showed splitting. (3) Although the vibrations in the ligands and their metal complexes were not the same, the pyrazine spectrum under pressure showed similarities to spectra of the corresponding metal complexes. This may appear to indicate that metallic complexation involves a pressure effect. The splitting of bands can be accounted for in terms of a lower symmetry or involving factor-group splitting. A new study of dihalocy-

clohexanes in the far IR region has recently appeared [200]. Pressure dependencies of the Raman and IR spectra of $\alpha$-, $\beta$-, $\gamma$- and $\delta$-octahydro-1,3,5,7-tetranitro-1,3,5,7-tetrazine have been made [201].

*(b) Metal sandwich compounds.* In a study on the effects of pressure (to 35 kbar) on the IR active skeletal vibrations of metal sandwich compounds, it was found that the $\nu(\text{M—ring})_{asym}$ vibrations are more sensitive to pressure than the ring tilt mode [202]. Table 21 shows the pressure dependencies in these compounds.

*(c) Metal—halogen stretching modes.* In complexes displaying both asymmetric and symmetrical metal—halogen stretching vibrations it was demonstrated that pressure effects (to 50 kbar) on the symmetrical vibration are more effective [203]. Although only minor shifts are observed, the symmetrical mode shows large decreases in intensity. The compounds studied included the following: 1. norbornadienedichloroplatinum(II), $(C_7H_8)PtCl_2$; 2. 2,2′,2″-terpyridinedichlorozinc(II), $(terpy)ZnCl_2$; 3. bis($\alpha$-picoline)dichlorocobalt(II), $(C_6H_7N)_2CoCl_2$; 4. tetraphenylarsenic trichlorostannate(II) $[(C_6H_5)_4As][SnCl_3]$; 5. tetraphenylarsenic trichlorogermanate(II), $[(C_6H_5)_4As][GeCl_3]$; 6. norbornadienedibromoplatinum(II), $(C_7H_8)PtBr_2$; 7. 2,2′,2″-terpyridinebromozinc(II), $(terpy)ZnBr_2$; 8. bis(pyridine)dibromocobalt(II), $(C_5H_5)_2CoBr_2$; 9. bis($\alpha$-picoline)dibromocobalt(II), $(C_6H_7N)_2CoBr_2$.

Results with the bromides indicate that the metal—bromine stretching mode behaves similarly to the metal—chlorine mode under pressure. However, since the assignments for the $\nu_{MBr}$ vibration are less well known because of the close proximity of the metal—nitrogen stretching vibration, further studies are necessary. Figure 16 shows the low frequency $\nu M—X_{asym}$ and $\nu M—X_{sym}$ vibrations $[\phi_4As][SnCl_3]$ as a function of pressure.

Lever has reported in a series of papers [204a] that metal—ligand vibrations in coordination complexes upon cooling to 80 K, increase in frequency relative to the "pure" ligand vibrations. The cooling effects are very similar to those observed with the application of high pressure (Sections (1)(a) and (1)(c)

TABLE 21

Pressure effects on skeleton modes of metal sandwich compounds [202]

| | Ring tilt ($cm^{-1}$) | | $\nu$(M-ring) ($cm^{-1}$) | |
|---|---|---|---|---|
| | Ambient pressure | 35 kbar | Ambient pressure | 35 kbar |
| $Fe(Cp)_2$ | 491 | 494 | 461 | 474 |
| $Ru(Cp)_2$ | 447 | 476 | 381 | 390 |
| $Mn(Cp)_2$ | 432 | 437 | 409 | 420 |
| $Cr(C_6H_6)_2$ | 487 | 491 | 453 | 475 |

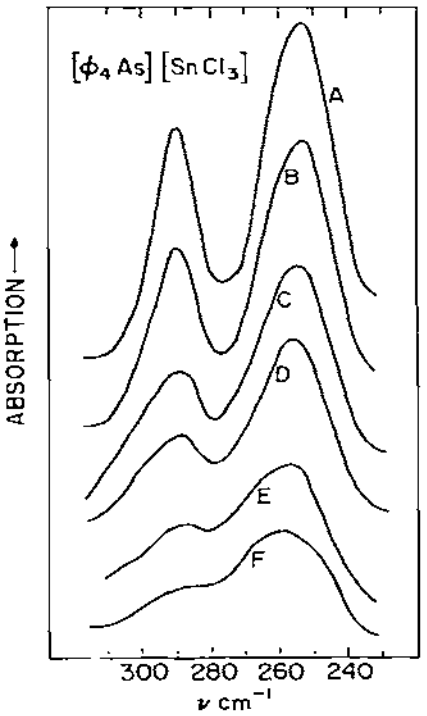


Fig. 16. Frequency of $\nu_{SnCl_{asym}}$ and $\nu_{SnCl_{sym}}$ in [$\phi_4$As][$SnCl_3$] as a function of pressure [203]. (Figure reproduced through the courtesy of the authors and the American Chemical Society, Washington, D.C.)

above). The use of low temperature has been suggested as a guide to band assignments in these complexes.

*(d) Metal—halide bridging vibrations.* Complexes of the type $CoL_2X_2$, where L = py, 4-Cl(py) or 4-Br(py) and X = Cl or Br are known to exist in polymeric and monomeric forms. The monomeric forms are tetrahedral and blue or green colored, and the polymeric forms are octahedral and lilac colored. The assignments for bridged cobalt—halide stretching vibration ($\nu_b$CoX) and terminal vibration ($\nu_t$(CoX) in these complexes were made possible by pressure studies to 28 kbar [204]. The $\nu_b$CoX vibrations manifested appreciable blue shifts as opposed to the $\nu_t$CoX vibration. The $\nu$(Co—N) shifts appear to be smaller, of the order of 18 cm$^{-1}$.

*(e) Complex compounds.* High pressure studies of some hexa-ammine complexes of Ni(II) and Co(II) have been made [205]. The pressure studies to 40 kbar for the Ni(II) complexes were different than low-temperature studies, and indicated a phase change and a lowering of symmetry being involved.

Complex halides like $K_2PtCl_4$, $K_2PdCl_4$, $K_2PtCl_6$ and $K_2PdCl_6$ have been studied at high pressure (ca. 33 kbar) [206]. In the $K_2MCl_4$ complexes of $D_{4h}^1$ symmetry [207] it was found that the $E_u$ internal vibrations were more pressure sensitive than the $A_{2u}$ internal vibration in the $MCl_4^{2-}$ ions. The most pressure sensitive external mode was the translational lattice mode along the long axis $a_0$, while the mode along the short axis $c_0$ was less pressure dependent. It was concluded that with an increase in pressure, contraction occurred along the $a_0$ axis, while a contraction or even expansion occurred along the $c_0$ axis. The X-ray work of Drickamer may lend some substantiation to these conclusions, as in the tetragonal solids $MnO_2$ and $SnO_2$ pressure contracts along the $a_0$ axis while the $c_0$ axis expands [172,173].

In the cubic crystals ($O_h^5$) $K_2MCl_6$, where M = Pt(II) or Pd(II), differentiation between internal and external modes was less certain, although the lattice mode appeared to be slightly more pressure sensitive. A series of transition-metal hexahalides was also studied under pressure to 20 kbar, and Adams and Payne [208] concluded that the pressure sensitivity followed the order $\nu_2 > \nu_4 > \nu_3$. For $M_2PtCl_6$, where M = K, Rb, Cs, Tl or $NH_4$, the pressure sensitivity of the $\nu$(Pt—Cl) modes of vibrations decreased in the order $A_{1g} > E_g > F_{1u}$ at pressures to 20 kbar [209].

Several complex cyanides have been investigated at high pressures up to 30 kbar, and the effects studied by IR spectroscopy [210]. The compounds examined were $K_2[Zn(CN)_4]$, $K_2[Cd(CN)_4]$, $K_2[Hg(CN)_4]$, $Zn(CN)_2$, $Cd(CN)_2$ and $Hg(CN)_2$. Pressure effects were studied by examining the CN stretching region as well as the metal—CN stretching region (200—600 $cm^{-1}$). For the $M(CN)_4^{2-}$ tetrahedra it was found that the degeneracy of the $F_2$ vibrations was removed with pressure. It was concluded that for M = Zn or Cd the symmetry had lowered to $D_{2d}$, while for M = Hg to $D_2$ or $C_{3v}$. Lower symmetry resulted for $Zn(CN)_2$. However, an increase in symmetry took place for $Hg(CN)_2$ and $Cd(CN)_2$.

A far IR study of salts of $SeX_6^{2-}$, where X = Cl or Br and $TeX_6^{2-}$ where X = Cl, Br or I at pressures up to 40 kbar was made [211]. All bands were observed to show blue shifts with the $\nu_4$ bending mode exhibiting the most dramatic effect. For some compounds which did not show $\nu_4$, the band appeared with increased pressure. In most cases which showed $\nu_4$ at ambient pressures, the vibration eventually disappeared with increased pressure. The results were explained on the basis of an anion—cation bonding scheme, which allows a pressure-dependent delocalization of the inert-pair electrons throughout the lattice.

*(f) Miscellaneous.* In a Raman study of metal carbonyls the $A_{1g}$ $\nu$(CO) shifted 12 $cm^{-1}$ at 25 kbar in tungsten carbonyls, while the $E_{1g}$ mode was substantially less sensitive [212].

*(2) Pressure effects on spin states*

A number of changes of oxidation state and spin states caused by pressure

have been reported by Drickamer and Frank [27]. In these cases Mössbauer or absorption spectroscopy was used as the diagnostic tool to observe the changes. For changes in solutions, see Sinn [26].

Recently, several systems have been examined using vibrational spectroscopy as the diagnostic tool to identify spin-state equilibria in the solid state. In these examples the far IR region, and in particular, the metal—ligand vibration was followed with pressure to determine a change from a high-spin to a low-spin state. The high-spin, metal—ligand vibration occurs at lower energy than the low-spin, metal—ligand vibration. In some instances low temperatures are used with pressure to facilitate the conversion.

The complex $NiBr_2(Bz\phi_2P)_2$ was converted at 12 kbar from a high-spin, distorted tetrahedral molecule to a low-spin, square-planar configuration [213]. In this complex a structural change as well as a spin-state conversion occurred. $Co(nnp)(NCS)_2$, where nnp = $Et_2N—(CH_2)_2—NH—(CH_2)_2P\phi_2$, was converted at 10 kbar and 150 K from the high-spin to low-spin state [214]. The relationship of the equilibria with temperature and pressure is shown below.

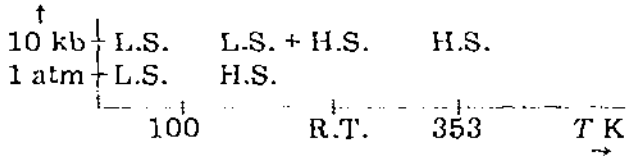


The $Fe(phen)_2X_2$ and $Fe(bipy)_2X_2$ complexes, where phen = 1,10-phenanthroline, bipy = 2,2'-bipyridine and $X = Cl^-, Br^-, N_3^-, NCO^-, OAc^-, HCOO^-$ exist in high-spin states [215]. The complexes $Fe(phen)_2(NCS)_2$, $Fe(phen)_2(NCSe)_2$ and $Fe(bipy)_2(NCS)_2$ were studied at high pressures and/or low temperature [215]. Complete conversion with pressure to low spin did not occur. However, the mixtures of high-spin and low-spin forms maintained at high pressures, could be converted to the low-spin state if the sample was cooled to 100 K. The high-spin state can be converted to the low-spin state directly with cooling to 100 K. The results parallel those obtained by Fisher and Drickamer [216] using Mössbauer techniques for $Fe(phen)_2(NCS)_2$ and $Fe(phen)_2(NCSe)_2$. High-spin—low-spin crossovers with pressure have also been observed for tri(N-ethyl-N-phenyldithiocarbamato)iron(III) [217,218], and represent the first pressure conversions of Fe(III) to low-spin. These results may have some consequences in problems relating to the earth's mantle.

The results of the low temperature conversion to low spin may be explained in terms of a strengthening of the Fe—N (phen or bipy) and Fe—N (NCS and NCSe) bonds due to back-donation of the $t_{2g}$ electrons of the metal to the $\pi^*$ orbitals of the organic ligand and NCSe. This mechanism may also be present at the outset of pressure applications, but the back-donation of the metal is reduced with increasing pressure by the accessibility of the $\pi$ electrons from the ligand to the ligand $\pi^*$ orbitals [27]. Table 22 summarizes high-pressure spin-state conversions.

TABLE 22

High pressure spin—spin interconversions [215—218]

| Compound | Central atom C.N. | High spin (No. of unpaired e's) | | Conversion pressure (kbar) | Experimental probe |
|---|---|---|---|---|---|
| Fe(NO)(salen) ($d^5$) | 5 | 3 | High Spin → Low Spin | 21 | NO stretching region |
| $Fe(phen)_2(NCS)_2$ ($d^6$) | 6 | 2 | High Spin → Low Spin | 18 | Skeletal-FIR |
| $Fe(phen)_2(NCSe)_2$ ($d^6$) | 6 | 2 | High Spin → Low Spin | 8—10 | Skeletal-FIR |
| $Fe(bipy)_2(NCS)_2$ ($d^6$) | 6 | 2 | High Spin → Low Spin | 15 | Skeletal-FIR |
| Co(nnp)$(NCS)_2$ ($d^7$) | 5 | 3 | High Spin → Low Spin | 4 | Skeletal-FIR |
| $Ni(Bz\phi_2P)_2Br_2$ ($d^8$) | 4 | 2 | High Spin → Low Spin [a] | 12 | Skeletal-FIR and electron regions |
| $Fe(EPDTC)_3$ ($d^5$) | 6 | 5 | High Spin → Low Spin | 35 | Skeletal-FIR |

[a] Structural conversion also occurs.

Abbreviations: phen = phenanthroline; bipy = bipyridyl; $nnp = Et_2N{-}(CH_2)_2{-}\overset{H}{N}{-}(CH_2)_2P\phi_2$; Bz = benzyl; $\phi$ = phenyl; salen = NN'-ethylenebis(salicylideneimine) = 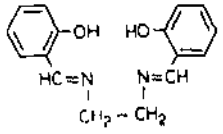

; EPDTC = N-ethyl-N-phenyldithiocarbamato.

*(3) Ligand isomerism*

Ligand isomerism is well characterized. Most of the studies have involved equilibria between the two forms in solution. Little is known of these equilibria in the solid state. In solid $Ni(en)_2(NO_2)_2$ at a pressure of 30 kbar, the violet form (obtained at ca. 120°C) was transformed to the red form [219]. The red isomer is the dinitro form, while the violet isomer is the dinitrito form. The 560 nm band was used to monitor the transformation.

*(4) Pressure reduction*

In a study at high pressure of $[(CH_3)_4N]_3[Fe(NCS)_6]$ (ref. 220) it was observed that a pressure-dependent reduction of Fe(III) to Fe(II) occurred, confirming the Mössbauer studies of Fung and Drickamer [221]. The reduction was characterized by the appearance of a new band at 238 $cm^{-1}$ at lower frequency than the 295, 270 $cm^{-1}$ vibrations attributed to the $\nu_{Fe-N} + 3_{-N}$ mode. A similar reduction [222] was found with pressure for $[Mn^{III}(CN)_6]^{3-}$ and $[Fe^{III}(CN)_6]^{3-}$ from a study of the $\nu_{CN}$ vibration in the $[M^{III}(CN)_6]^{3-}$ species. No evidence was obtained, which could be attributed to any ligand isomerization occurring.

Other oxidation—reduction effects of pressure using Mössbauer techniques have been noted by Drickamer and Frank [27].

*(5) Structural conversions with pressure*

Most structural interconversions have been studied in solution. NMR spectroscopy has been an ideal tool for such studies because often the equilibrium established between labile structures can be shifted in favor of one structure by a change in temperature. Until recently, few high-pressure studies of solid-state structural interconversions of complexes have used vibrational and electronic spectroscopy. The Mössbauer effect has, however, been used extensively by Drickamer and Frank [27].

It is reasonable to assume that solid-state interconversions involve considerably larger energy effects than those observed in solution. For solid complexes, in addition to the symmetry effects discussed above, molecular packing, lattice forces, ligand flexibilities, metal—ligand bond distances, *d—d* electronic transition energies, orbital overlap and orientation effects, and hydrogen bonding among other factors must also be considered. High pressure is known to affect many of these factors [27,223,224] and will favor the structure with a smaller packing volume. High-pressure effects are observed to shorten the metal—ligand bond distance and to increase the average ligand field strength [223—225]. In the cases involving high-spin complexes, this increase in ligand field energy may be sufficient to overcome the electron spin pairing energy and produce a low-spin complex.

Of particular interest is the effect of high pressure on the IR absorption bands of a solid complex. A reduction in the metal—ligand bond distance shifts the vibrational bands to higher energy. For bending modes, which might possibly transform one structure into another, the effects of pressure

may be smaller and conceivably the associated band may shift to a lower energy. It is also possible that, at high pressure, normally forbidden modes may become allowed (in a lower site symmetry), and if this mode yields a structural interconversion, the vibration may then become allowed. Thus, it is of interest to examine the solid-state rigidity of various molecules with differing stereochemical configurations at high pressure.

*(iv) High-pressure studies of several solids in different symmetries*

Solid-state structural transformations obtained for several representative solids at high pressure are presented in Table 23. From these results, it may be concluded that structural interconversions are possible for transition-metal complexes in the solid state. The interconversions are all reversible, with the exception of that for the $Ni(Qnqn)Cl_2$ complex.

We have proposed a new scheme for the classification of the types of behavior observed in transition-metal compounds at high pressure (see Table 24) [226]. The four behavior classes are based primarily upon the presence or absence of a structural and/or electronic change in the complex between ambient and high pressure. Class 1 compounds exhibit neither large structural nor electronic changes, but they would include compounds which show small effects, such as slight unit cell contractions, minor crystallographic changes in space group, small changes in crystal-field parameters, and small shifts in charge-transfer bands. Class 2 compounds exhibit significant structural changes with, at most, minor electronic changes, whereas the reverse situation holds for class 3 compounds. Classes 2 and 3 may be further subdivided as shown in Table 24 depending upon the absence or presence of a coordination number change, etc. Class 4 includes compounds with both electronic structural changes at high pressure and, of course, could have many subdivisions if necessary based upon the presence or absence of each electronic and structural factor.

The behavior of various selected transition-metal complexes at high pressure will now be discussed in terms of their coordination number and behavior type.

*(1) Four-coordinate complexes*

The two complexes, dichloro- and dibromobis(benzyldiphenylphosphine)-nickel(II), $Ni(BzPh_2P)_2X_2$, may each be prepared as both red and green isomers [237]. Both of the red complexes are the diamagnetic square-planar forms of the complex. However, there are substantial differences between the two green isomers. The green bromide isomer (with a reduced magnetic moment of 2.70 $\mu$B at room temperature) has been shown by single-crystal X-ray analysis [238] to contain one square planar and two tetrahedral nickel atoms per unit cell. The magnetic moment of the green chloride isomer (3.23 $\mu$B at room temperature) and its spectroscopic properties reveal that it is fully tetrahedral in coordination geometry.

TABLE 23

Solid state structural transformations induced by high pressure [226]

| Compound | C.N. | Symmetry [a] ambient pressure | Structural transformation with pressure | Transformation press. (kbar) | Spectroscopic probe | Remarks |
|---|---|---|---|---|---|---|
| $Ni(Bz\phi_2P)_2Cl_2$ | 4 | Pure $T_d$ | No change | | Electronic FIR | |
| $Ni(Bz\phi_2P)_2Br_2$ [b] | 4 | 1/3 Planar (Square) 2/3 $T_d$ | Planar (square) | 20 | Electronic FIR | Reversible |
| $Ni(Qnqn)Cl_2$ | 4 | Distorted $T_d$ | Binuclear, SQP $[Ni(Qnqn)Cl_2]_2$ | 2 | Electronic FIR | Irreversible |
| $CuCl_4^{2-}$ [c] | 4 | Flattened $T_d$ | Planar (square) | 20 | FIR | Reversible |
| $Ni(CN)_5^{3-}$ [d] | 5 | SQP + TBP | SQP | 7 | IR in 4 μm | Reversible |
| $[NiLX]^+$, $NiLX_2$, $[NiL_2X]^+$ $NiL_3X_2$ | 5 | SQP + TBP | TBP | Onset of press. | Electronic | Reversible |

[a] Local symmetry around central metal atom considered. [b] $Ni(Bz\phi_2P)_2I_2$ inferred to be similar $Ni(Bz\phi_2P)_2Br_2$ from magnetic moment. [c] Cation is $(CH_3)_2CHNH_3^+$ or $Cs^+$. [d] Cation is $Cr(en)_3^{3+}$; compound is $\{Cr(en)_3Ni(CN)_5\}$ 1.5 $H_2O$.

Abbreviations: Bz = benzyl; $\phi$ = phenyl; Qnqn = *trans*-2-(2′-quinolyl)methylene-3-quinuclidione; L = organic ligand; X = halogen or pseudo halogen; $T_d$ = tetrahedral; SQP = square pyramidal; TBP = trigonal bipyramid.

TABLE 24

Behavior classes for pressure-induced solid-state changes [226] [a]

| Behavior class | Structural change | | Electronic change | | Examples | Ref. |
|---|---|---|---|---|---|---|
| | Geometric change | C.N. change | Spin-state change | Oxidation state change | | |
| 1 | No | No | No | No | Green $Ni(BzPh_2P)_2Cl_2$ | 213 |
| | | | | | $[Ni(Qnqn(Cl_2]_2$ | 227 |
| | | | | | $Co(Qnqn)Cl_2$ | 225 |
| | | | | | $FeS_2$ | 228 |
| 2A | Yes | No | No | No | Several $CuCl_4^{2-}$ | 229, 230 |
| | | | | | $Ni(CN)_5^{3-}$ | 231 |
| 2B | Yes | Yes | No | No | $Ni(Qnqn)Cl_2$, $Co(py)_2Cl_2$ | 204, 227 |
| 2C | Yes | No | Yes | No | Green $Ni(BzPh_2)_2Br_2$ | 213 |
| 3A | No | No | Yes | No | $Mn(Fe)S_2$ | 232 |
| | | | | | $Fe(phen)_2(N_3)_2$ | 216 |
| | | | | | $Fe(phen)_2(NCS)_2$ | 215, 216, 233 |
| 3B | No | No | No | Yes | $Fe(acac)_3$ | 234 |
| | | | | | $Cu(OXin)_2$ | 235 |
| | | | | | Hemin | 27 |
| 4 | Yes | | Yes | | $Co(NO)(Ph_2CH_3P)_2Cl_2$ | 236 |

[a] A modified version of that in ref. 226 appears above.
Abbreviations: C.N. = coordination number; Bz = benzyl; Qnqn = *trans*-2-(2′-quinolyl)methylene-3-quinuclidione; py = pyridine; ArgH = $(H_2N)_2CNH(CH_2)_3CHNH_2COO^-$; acac = acetylacetonate; OXin = 8-hydroxyquinoline.

Both the electronic and IR absorption spectra of the two paramagnetic green isomers were studied as a function of pressure [213]. The green $Ni(BzPh_2P)_2Cl_2$ isomer retains its tetrahedral coordination geometry at all pressures and shows no indication of any conversion to a square-planar geometry at high pressure. However, the green $Ni(BzPh_2P)_2Br_2$ isomer is transformed from the above-mentioned mixture of tetrahedral and square-planar coordination geometries at ambient pressure, to the purely square-planar red isomer at high pressure [213]. This reversible pressure-induced structural transformation is essentially complete at ca. 20 kbar and represents class 2C behavior. In this instance, the change in the spin state of the nickel ion occurs as a result of the geometric structural change and not directly as a consequence of the high pressure.

In another high-pressure study [227], it was possible to irreversibly convert the paramagnetic violet pseudotetrahedral nickel complex, $Ni(Qnqn)Cl_2$, into its yellow paramagnetic binuclear $[Ni(Qnqn)Cl_2]_2$ isomer. In these complexes, the Qnqn ligand is *trans*-2-(2′-quinolyl)methylene-3-quinuclidinone.

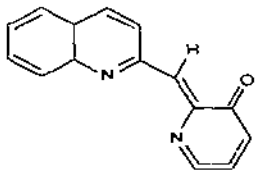

Qnqn

Both the yellow and violet isomers have been prepared directly [227], and the X-ray structure [239] of the yellow binuclear isomer has revealed two bridging and two terminal chlorine ligands and bidentate coordination for Qnqn. The application of pressure to the violet monomeric complex causes the two nickel—chloride nonbonded distances to decrease to a point where the two additional bridging chlorine bonds are formed, and the yellow binuclear complex results. The spectrum of the complex clearly reveals the irreversible changes in both the $\nu_{Ni-Cl}$ and $\nu_{Ni-N}$ vibrational bands as a function of pressure. The electronic absorption spectrum of the violet isomer also reveals the expected changes in the $d$—$d$ bands at high pressure.

This is the first example of such an irreversible pressure-induced structural transformation known to us. The irreversibility of this transformation may result from the bond energy of the two additional chlorine bridging bonds, which would make the reverse transformation thermodynamically unfavorable. This transformation involves both a change in coordination number and a change in coordination geometry and represents class 2B behavior. The yellow dimeric $[Ni(Qnqn)Cl_2]_2$ exhibits only minor changes at high pressure and is in class 1 [226,227].

The room-temperature preparation of $[(CH_3)_2CHNH_3]_2CuCl_4$ has been found [240] from X-ray studies to contain one copper ion in a square-planar configuration and two copper ions arranged in tetrahedrally distorted configurations. The crystal is held together by hydrogen bonding from the isopropylammonium ions. At high pressures the coordination geometry of the two tetrahedrally distorted copper ions is reversibly converted to a square-planar geometry [229]. The conversion is observed as a change in the $\nu_{Cu-Cl}$ and $\delta_{ClCuCl}$ vibrational bands. Confirmation for the conversion was also found in the change occurring in the electronic region [229,230]. A similar structural conversion is also found [230] in $Cs_2CuCl_4$ and $Cs_2CuBr_4$. These compounds exhibit a geometric structural change with no change in coordination number or spin-state and belong to class 2A.

*(2) Five-coordinate complexes*

An X-ray diffraction study [241] of the $[Cr(en)_3][Ni(CN)_5] \cdot 1.5\ H_2O$ com-

plex has shown that its unit cell contains two crystallographically independent $[Ni(CN)_5]^{3-}$ ions, one with a regular square-pyramidal geometry, and one with a distorted trigonal-bipyramidal geometry. Dehydration of the complex converts all of the $[Ni(CN)_5]^{3-}$ ions to the square-pyramidal geometry [241]. When this compound was subjected to pressures of ca. 7 kbar at 78 K, the coordination geometry of the trigonal-bipyramidal $[Ni(CN)_5]^{3-}$ ion was converted reversibly to the square-pyramidal geometry [231]. The IR spectrum of this compound at ambient and high pressure is presented in Fig. 17. In order to prevent the dehydration of the complex at high pressure (presumably a result of localized heating produced by the 6X beam condenser used with the pressure cell) these studies were made at 78 K. In this complex, the reversible transformation represents behavior class 2A in a five-coordinate complex.

An extensive high-pressure study of many five-coordinate nickel(II) complexes with ligands ranging from monodentate to tetradentate has revealed several nonrigid structures in the solid state [223]. The results for several metal ions are presented in Table 25 and reveal that "tripod-like" tetradentate ligands prefer the trigonal-bipyramidal structure. The importance of the larger number of chelate rings, and the increased entropy and free energy of formation for tetradentate ligand complexes of the type [NiLX] Y, are indicated by the more numerous trigonal-bipyramidal structures. As the number of chelate rings is reduced, stability decreases, and the tendency to form intermediate five-coordinate complexes results [242]. $NiL_3X_2$ complexes with no chelate rings are unstable and dissociate in solution, whereas the application of high pressures tends to distort these solids toward the distorted intermediate five-coordinate geometry. In these five-coordinate complexes, a gradual change from class 1 behavior (with small values of $d\nu/dp$) to class 2A behavior is observed.

The five-coordinate square-pyramidal complex Fe(NO)(salen) (salen = N,N'-ethylenebis(salicylidenimine)) has been shown to contain iron in an intermediate spin state ($S = \frac{3}{2}$) and to exhibit spin equilibrium at low temperature [243]. Mössbauer spectral results indicate that the complex most likely contains Fe(III) and $NO^-$, although this formulation is still open to question. A recent study of the NO vibrational absorption band as a function of pressure has revealed a shift to lower frequency at high pressure [244]. These results appear to be consistent with a change in spin state for the iron ion. This compound would appear to fit into class 3, but additional studies will be required to confirm and refine this classification because structural changes may also be significant.

Two isomers of $Co(NO)(Ph_2CH_3P)_2Cl_2$ are known [245]. One of these isomers is trigonal bipyramidal and contains Co(I) and $NO^+$ ions, most probably with a linear Co—N—O bond. The second isomer is square pyramidal and contains Co(III) and $NO^-$ with a bent Co—N—O bond. The NO vibrational absorption band occurs at ca. 1750 $cm^{-1}$ in the first isomer and at ca. 1650 $cm^{-1}$ in the second. A preliminary study indicates the structural conversion of the trigonal-bipyramidal isomer to the square-pyramidal isomer at high pressure

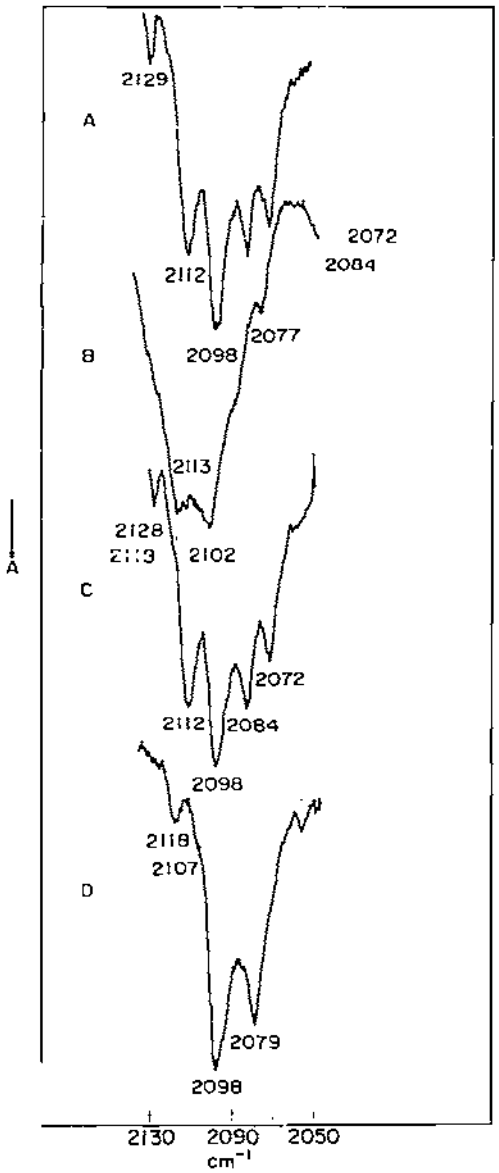


Fig. 17. The cyanide stretching vibrational bands in $[Cr(en)_3][Ni(CN)_5] \cdot 1.5\ H_2O$: A, at 78 K and ambient pressure; B, at 78 K and ca. 7 kbar; C, at 78 K and ambient pressure after release of high pressure. Spectrum D is that of $[Cr(en)_3][Ni(CN)_5]$ at ambient temperature and pressure [249]. (Figure reproduced through the courtesy of the authors and the American Chemical Society, Washington, D.C.)

TABLE 25

Structural inferences from pressure effects for several Ni(II), Pd(II), Pt(II) and Co(II) complexes containing ligands varying from tetradentate to monodentate [223]

| Complex [a] | Type of ligand | $d\nu/dp$ ($cm^{-1}$ $kbar^{-1}$) | Structure |
|---|---|---|---|
| [NiLX]Y (24) | Tetradentate | 33—70 | TBP |
| [PdLX]Y (2) | Tetradentate | 33—61 | TBP |
| [PtLX]Y (1) | Tetradentate | 27 | TBP |
| [CoLX]Y (1) | Tetradentate | 7 | SQP |
| [$NiLX_2$] (3) | Tridentate | 9—32 | Distorted, TBP-SQP |
| [$NiL_2X$]Y (5) | Bidentate | 9—32 | Distorted, TBP-SQP |
| [$CoL_2X$] (2) | Bidentate | Very slight shift | SQP |
| [$NiL_3X_2$] (6) | Monodentate | 8—29 | Distorted, TBP-SQP |
| [$CoL_3X_2$] (2) | Monodentate | 8—23 | Distorted, TBP-SQP |

[a] Numbers in parentheses indicate number of compounds studied.
Abbreviations: TBP = trigonal bipyramid; X = halide or pseudo-halide ion; SQP = square pyramid; Y = polyatomic anion.

[236]. This represents class 4 behavior with significant structural and electronic changes.

*(3) Six-coordinate complexes*

To date we have not been successful in changing the coordination number or geometry of an octahedral (or close to octahedral) complex at high pressure. However, several octahedral high-spin complexes have been reversibly converted, at least in part, to the analogous low-spin octahedral complexes at high pressure [215,216,246,247]. Table 22 summarizes some of these results. The initial conversion from the high-spin to the low-spin state has been explained [27,216] by the increase in ligand-field potential with pressure until it exceeds the electron pairing energy. This initial effect is accompanied by the back-donation of the metal $t_{2g}$ electrons into the $\pi^*$ orbitals of the ligand. With a further increase in pressure this back donation is reduced by the accessibility of $\pi$ electrons from the ligand [27].

*(4) Nonrigidity of solids at high pressure*

It may be concluded that solid-state high-pressure structural transformations are possible in transition-metal complexes. All of the transformations examined thus far have been reversible, with the exception of that in Ni(Qnqn)$Cl_2$, in which a dimer is formed at high pressure. In this complex, two additional bonds are formed on dimerization, and they contribute to the stability of the high-pressure phase.

The probability of producing structural interconversions with pure or nearly pure tetrahedral and octahedral complexes is predicted, on the basis

of the theoretical considerations discussed [197,198], to be small. For undistorted tetrahedral complexes, this prediction is borne out by experiment. Attempts [248] to convert complexes of nearly tetrahedral symmetry have been unsuccessful. The results of our work, however, indicate that the pressure-induced conversions of tetragonally distorted tetrahedral complexes are possible, in particular where an asymmetric ligand field is observed by the central atom (e.g., a complex involving several types of ligands). The importance of a distorted structure appears to be a necessity in a solid-state pressure conversion [249].

It is possible that distorted six-coordinate complexes may also behave similarly [250—252]. The results observed to date for four- and six-coordinate complexes are not surprising because the energy barrier to rearrangement for true tetrahedral and octahedral structures is certainly high. For the $Ni(BzPh_2P)_2Br_2$ complex, the unpaired electrons may contribute to the lowering of the energy difference between the distorted tetrahedral and the square-planar configurations. This effect would be superimposed upon the beneficial effect of a starting structure which is distorted toward the square-planar geometry.

For five-coordinate complexes the energy barrier for structural interconversion is small, and many examples have been reported in which the trigonal-bipyramidal and square-pyramidal isomers both exist [246,253—257]. This is apparently also true in the solid state, because our high-pressure studies indicate that interconversion is readily obtained. In systems containing a tripod-like tetradentate ligand, the ligand flexibility favors the trigonal-bipyramidal structure. For the $Ni(CN)_5^{3-}$ ion, a structure which is distorted in the direction of the pressure-stable square-pyramidal phase, the monodentate cyanide ion permits the rearrangement to occur.

Nonrigid configurations for seven- and eight-coordinate complexes have been demonstrated in solution studies [258—269]. However, no solid-state high-pressure studies have been reported to date.

Recent studies have disclosed pressure effects on solids which are interesting and surprising [270,271]. Copper(II) and nickel(II) complexes of N,N-diethylethylenediamine, N,N-dimethylethylenediamine and C,C-dimethylethylenediamine of the type $M(L)_2X_2$ where X = anion, have been found to be reversibly thermochromic [271a]. The Lever effect has been advocated as the mechanism for the thermochromism, axial interactions between the anions and the $M—N_4$ plane increase with temperature and metal—nitrogen distances are expanded. Axial interaction causes an increase in coordination number from 4 to 6, accompanied by a color change. The reverse occurs with an increase in pressure, and axial interactions are at a minimum, maintaining the four-coordinate state.

A pressure study involving $MCl_4^{2-}$ ions was made using counter ions which were capable of hydrogen bonding and those which were incapable [272]. It was found that hydrogen bonding stabilizes an octahedral geometry for $Mn^{2+}$ and $Fe^{2+}$. With $Ni^{2+}$, preparations in solution gave $RNiCl_3$ complexes which

TABLE 26

Summary of pressure effects on $R_2MCl_4$ complexes [272]

| Counterion [b] | Mn(II) $d^5$ | Fe(II) $d^6$ | Co(II) $d^7$ | Ni(II) $d^8$ | Cu(II) $d^9$ |
|---|---|---|---|---|---|
| $R_4N^+$ | $T_d$ | $T_d$ | $T_d$ | $T_d$ | $D_{2d}$ |
| $R_3NH^+$, $R_2NH_2^+$, $RNH_3^+$ | Increasing internal pressure | | | | |
| | $O_h$ | $O_h$ | $D_{2d}$ | $O_h$ [a] | $D_2$ and $D_{2h}$ |
| $R_3NH^+$, $R_2NH_2^+$, $RNH_3^+$ | Increasing internal pressure | | | | |
| | | | $D_{2d}$ | | $D_{2h}$ |

[a] Stoichiometry involves $NiCl_3^-$ from solution; from melt [272] polymeric octahedral structures are obtained with a stoichiometry of $[R_2NiCl_4]_x$. [b] R = alkyl group.

contain $NiCl_6$ octahedra, and polymeric octahedral complexes with the stoichiometry $(R_2NiCl_4)_x$ from melts. Table 26 summarizes the results of pressure effects on $R_2MCl_4$ complexes.

### F. GEOLOGICAL APPLICATIONS

The interior of the earth is at high temperature and under megabar pressures. In our discussions heretofore we have stressed changes in molecules created at kbar pressures. It is of the utmost importance to be able to know what major physical and chemical changes occur to matter at megabar pressures. Since the composition of the core and the mantle involve, besides silicates, transition metal minerals, mostly iron and nickel, effects of Mbar pressures and high temperatures on these substances is of obvious interest. It would be expected that transition chemistry under these conditions would be different than under ambient conditions. Changes in oxidation state, spin state, coordination numbers, and absorption properties with pressure and temperatures affect the density, magnetic, electrical and thermal properties of the earth's interior. It is of interest to geochemists and to geophysicists to simulate conditions in the laboratory to make $p$ and $t$ studies on minerals. New concepts of the earth's constitution, evolution and properties depend on these studies, and the interpretation of the results. This research would serve to answer many questions which still remain unanswered concerning our own planet, and could serve as an aid in explaining the behavior of other planets. Studies at high temperature and Mbar pressures are now possible, and have commenced. The necessary experimental tools to accomplish this are now available (see Section B). X-ray, Mössbauer and visible measurements have been made with the Mbar cell of Mao and Bell [289,297,303]. Vibrational spectroscopy may play a role in these applications in the future. However, the present construction of the cell may restrict its use in the IR region, because

of the severe energy requirements and the need to accommodate a beam condenser [273]. However, it is possible that new instrumentation involving tunable diode lasers in the IR may overcome these difficulties.

Many of the original studies to attempt to create Mbar pressures were done with shock waves [274]. As previously stated, this is a rather difficult and destructive way to study the problem. Modern techniques using the diamond anvil cell to Mbar pressures and 3000°C are now available, and this should provide impetus to this field.

Table 27 shows some examples of early general results or effects of $t$ and $p$ (50 kbar or less) on minerals. Transformation of minerals with $t$ and $p$ indicate that few minerals found on the surface would be stable in the deep interior of the earth, an observation made by Bridgman in 1945.

The effects of $t$ and $p$ on interatomic distances in oxygen-based minerals have been reported [298,299]. Mechanisms of Si(IV) to Si(VI) in silicate minerals have also been determined [300]. Other mineral studies have also appeared recently in the literature [301,302].

Some more recent studies of minerals at higher pressure are outlined in Table 28. Ming and Bassett [296] have found from their $t$ and $p$ studies that at 250 kbar and 1000°C ferromagnesium silicate breaks down to the simple oxides of iron, magnesium and silicon. In the interior of the earth, below 650 km, it is believed that these oxides constitute the main mineral constituents in the mantle. The presence of iron oxides is of considerable interest since they play a major role in determining the optical, electrical and thermal properties of the mantle as well as in the evolution of the earth.

An interesting result of studies at high pressure and temperature were those of Bell et al. [297]. Studying iron-rich basaltic glass at 100—150 kbar and ca. 2000°C they showed that the ferrous-bearing compounds would disproportionate into a ferric iron phase plus a metallic iron phase. Thus, both a highly oxidized crust and a metallic core can coexist and can be simultaneously formed, obviating some early evolutionary history of earth. The results lend support to the fact that the core and mantle may exist in a chemical equilibrium.

TABLE 27

Some mineral transformations at relatively low pressures

| | Temp. (°C) | Pressure (kbar) | Ref. |
|---|---|---|---|
| β-Quartz = α-quartz | 573— 800 | 24 | 275 |
| α-Quartz = coesite | 400— 600 | 10 | 276, 277 |
| | 700—1700 | 20 | 278 |
| Sillimanite = kyanite | 1000—1500 | 5 | 279, 280 |
| Albite = jadeite + quartz | 600—1000 | 50 | 281 |
| Fayalite = spinel | | 25 | 282, 283 |

TABLE 28

Transformation of several minerals at high temperatures and pressures [296]

| Mineral | Pressure (kbar) | Temp. (°C) | Products | Ref. |
|---|---|---|---|---|
| $FeSiO_3$, ferrosilite | 95 | 1000 | $Fe_2SO_4 + SiO_2$, stishovite | 284 |
| $(Fe, Mg)SiO_3$, clinopyroxene | 80—180 | 1000 | $(Fe, Mg)_2SiO_4$, spinel + $SiO_2$, stishovite | 285, 286 |
| $MgSiO_3$, clinoenstatite | 200—280 | 1000 | $Mg_2SiO_4$, $\beta$-phase + $SiO_2$ stishovite | 287 |
| $\beta$-$Mg_2SiO_4$ | >280 | 1000 | $\gamma$-$Mg_2SiO_4$, spinel | 287 |
| $Fe_2SiO_4$, spinel | 250 | 1000 | $FeO + SiO_2$, stishovite | 288, 289 |
| $(Mg, Fe)_2SiO_4$, olivines | 50—150 | 1000 | Spinel, $\gamma$-phase | 290—294 |
| $Mg_2SiO_4$, fosterite | 330 | 1000 | $MgO + SiO_2$, stishovite | 295 |
| Complex basalt | 100—150 | 2000 | $Fe_2O_3$ + Fe | 297 |

Minerals containing iron, such as olivine and spinel, under pressure, appear to indicate that a marked increase in conductivity occurs with pressure in excess of 100 kbar [303]. Similar results have been indicated with other solid phases approaching metallic behavior with pressure. In addition, charge transfer properties change in these minerals due to pressure effects on electronic orbitals [286]. These effects bear heavily on the earth's internal temperature and electrical conductivity, as well as on models of earth formulated to date. The question of whether the thermal conductivity in earth is radiative or conductive may, in part, have been answered in the Bell et al. [297] experiment. Both iron and ferric oxides are opaque to thermal radiation, but have high thermal conductivities.

We have only attempted to briefly indicate some geological applications of T and P. Further discussions are available in several reviews [274,303,304], and other reports [305—307].

## G. SUMMARY

A summary of the solid state pressure effects discussed in the previous sections follows.

### *(i) Structural transformations*

We have discussed a number of structural transformations that occur in the solid state under pressure. These are summarized below. (1) Phase changes in alkali metal halides, rare earth monochalcogenides from NaCl to CsCl structure where C.N. 6 → 8. (2) Transitions occurring in minerals where C.N. 4 → 6. (3) Transitions to metallic state, e.g., rare earth monochalcogenides, iodine,

solid hydrogen, xenon. (4) Transformations in coordination compounds. The various types of transformations are listed in Table 24. It may be noted that some structural changes occur with an increase in coordination number, and others occur with no change.

*(ii) Effects on vibrational transitions*

Four types of pressure-sensitivity for molecular vibrations have been observed thus far in the course of pressure studies on various modes of vibrations: (1) a broadening and a decrease in peak intensity of vibrations; (2) the doubling of absorption bands; (3) the splitting of degenerate vibrations; (4) frequency shifts in bands. Some of these effects have been observed for both external and internal vibrations.

*(1) External vibrations*

The effects of pressure on external vibrations have been demonstrated. Both the longitudinal and transverse optical modes are seen to shift in compressible ionic solids. In all cases studied thusfar, the shift is in the direction of higher frequency in agreement with low-temperature shifts. However, the pressure shifts may be considerable when compared with the temperature shifts. It is known that the temperature dependence of the peak position and half-width of lattice vibrational modes consist of two contributions: (1) the purely volume-dependent contribution; and (2) the contribution from the various anharmonic (cubic and higher) terms in the potential energy of the lattice. Often the directions of shifts in the temperature dependence experiment may be opposite to each other, resulting in a cancellation, and a small overall shift. For example, the specific volume of $\alpha$-quartz shows only a 0.3% decrease from room to liquid-air temperatures [308], and this is smaller than the change occurring upon compression from ambient pressure to 4 kbar [309]. Such pressure studies may provide useful information on the amount of anharmonicity existing in solids of this type. Further, it should be possible in some cases to obtain compressibility data in compressible solids from pressure-frequency measurements (see eqn. (1)). Molecular lattices show similar pressure effects [79].

In addition to the spectral blue shifts, lattice vibrations will broaden and diminish in peak intensity. This appears to be characteristic of all types of vibrations. No quantitative studies have been made to determine the effect of pressure on the integrated intensities of these vibrations. This may prove to be very difficult, since results may not be reproducible because of the pressure gradient existing across the diamond anvil faces. The broadening effects may be connected in part with this pressure gradient, since Raman studies in a hydrostatic cell do not show this pressure broadening of lattice bands [79,159].

The blue shifts of ionic or molecular lattice modes may result from the contraction of the solid under pressure, causing interionic and intermolecular

distances to shorten [48,167,310,311]. The large pressure effects on compressible lattices are related to the small repulsive forces present in the neighboring ions or molecules.

*(2) Internal vibrations*

Earlier work indicated that internal modes are affected by pressure, but in a much less dramatic way than the external modes. Frequency shifts are generally small in most cases, either in a blue or red direction. In hydrogen-bonded compounds, studies of the O—H stretching vibration indicated spectral red shifts [48,310]. Red shifts were also observed for $HgCl_2$ and its dioxane complex by Mikawa et al. [145]. In most of our pressure studies with internal modes, blue shifts have been observed.

The broadening of bands and decreased peak intensities also occur with pressure. In some cases the symmetrical stretching vibration ($A_1$ species) is found to be particularly sensitive to pressure [203]. This compares favorably with the findings of Nedungadi [312], who studied the temperature dependence of $\alpha$-quartz and found that the most sensitive vibration was an $A_1$-type mode. Pressure dependencies of $\alpha$-quartz produced similar results with the $A_1$ frequencies more sensitive than the $E$-type vibration [313]. Again, it must be inferred that not all $A_1$ vibrations are pressure sensitive, as $A_1$ bending vibrations and certain $A_1$ stretching vibrations are not particularly affected at higher frequencies.

Other pressure effects have recently been demonstrated. The $\nu_4(F)$ bending vibration in $KMnO_4$, which is already split into two bands at ambient conditions, proceeds to lose all of its degeneracy with pressure. Studies with ligand ring vibrations in the mid-IR region have demonstrated that one can also obtain a doubling of vibrations with pressure [199]. An attempt to explain these results, at least qualitatively, follows.

*(a) Sensitivity of $\nu_1$ stretching vibration to pressure.* The sensitivity of the $\nu_1$ stretching vibration in various compounds (inorganic and coordination compounds) is especially interesting. By contrast, a symmetrical bending vibration of type $A_1$ may not be particularly affected (Fig. 16 illustrates the sensitivity of the $A_1$ species in the metal—chloride stretching region). The intensity of the symmetrical stretch has practically disappeared with pressure, while the asymmetric stretch, although less intense, is still readily observed.

This $\nu_1$ vibration involves an expansion of molecular volume, and these "expansion vibrations" are particularly sensitive to pressure [203]. In addition, the dipole moment change for the vibration apparently decreases and this causes a decrease in the intensity. The actual mechanism as to how this is accomplished is obviously unknown at present. Since the intermolecular distances are being diminished, it may be possible to change certain bond angles while the material is under external stress. If the bond angles increase and approach 180°, the dipole moment change for the vibration might approach zero. Carbon dioxide is a case in point, where the bond angle

O—C—O is 180° and the $\nu_1$ vibration is forbidden in the IR spectrum. However, it is observed in the Raman measurements and it would be interesting to observe similar molecules in the Raman experiment with pressure. Water, with a bond angle of ca. 104°, shows an IR-active $\nu_1$ vibration.

*(b) Splitting of degenerate vibrations.* The loss of the degeneracy of *E* or *F* type vibrations with pressure is possible. In some cases this may be due to a lowering of symmetry of the molecule. In other cases, where a molecule may have two or more molecules per unit cell, it is possible that the vibrations in the unit cell might couple, causing a factor group splitting (Davydov splitting) [314].

*(c) Doubling of absorption bands.* In the course of various studies [199] it has been observed that a doubling of bands occurs with pressure. This may be due to a lowered site symmetry induced in the solid state by the external pressure. Alternatively, two accidentally overlapping vibrations may occur at the same frequency. These may be induced to separate because of a difference in the pressure dependencies manifested by the two vibrations. Alternatively, this may be caused by factor group splitting.

*(d) Lack of frequency shift for internal modes.* The lack of large frequency shifts for most internal modes in polyatomic compounds is a very useful consequence, for it may allow one to distinguish between such a vibration and a lattice mode in a compressible solid. The lack of larger shifts is related to the stronger repulsive forces present in the atoms of these molecules. However, it is dangerous to extrapolate that all internal modes will behave in this manner. The electron density around the various atoms involved may be a very important factor. As the pressure is increased and the atoms or molecules approach each other, the interaction of the electron field increases. For simpler molecules with minimal electronic interaction, such as hydrogen, it may be possible for considerable shifts in frequencies of the internal mode to occur; however, as the electronic fields become more and more complex, the repulsive forces increase and the shifts decrease. Vu et al. [315] demonstrated that a shift of ca. 1 $cm^{-1}$ $kbar^{-1}$ occurs for the pressure-induced $\nu_{H-H}$ vibration in solid hydrogen. A somewhat lower pressure dependence is found for HCl [316].

*(iii) Functional approach to explain pressure effects*

Recently, Gutmann and Mayer [317] have attempted to explain pressure effects on materials using the functional approach. This is based on a model which considers that pressure acts by increasing the electron donor properties of parts of the systems. In many ways pressure may be considered to play the role of an electron donor. In this way, some of the pressure effects on molecules may be explained.

## H. MISCELLANEOUS

Several new pressure conversions of gases to a metallic state are possible in view of existing high-pressure instrumentation. For a discussion on metallic hydrogen, see refs. 318—323. For the possible conversion of xenon to a metallic state, see Ruoff and Nelson [324]. Many of the aforementioned physical tools used with the DAC, including electronic and vibrational spectroscopy, may play a role in the analyses and characterization of these possible new metallic phases.

## ACKNOWLEDGEMENTS

The author wishes to express his thanks and appreciation to Professor Luigi Sacconi for the invitation to present lectures in Italy, which triggered this review; to the Italian Research Council for a portion of the funding; to NATO for other portion of funding; to Argonne National Laboratory and the U.S. Department of Energy for their approval of the travel. Special thanks to Drs. Louis J. Basile (ANL), C. Postmus (North Park College, Chicago, Illinois), K. Nakamoto (University of Marquette), S.S. Mitra (University of Rhode Island), and Mr. Anthony Quattrochi (U.S. Tabacco, Franklin Park, Illinois), for their contributions to many of the results reported in this paper. Last but not least, thanks to the university faculty and students who participated.

## REFERENCES

1 E.H. Amagat, Ann. Chim. Phys., 29 (1893) 68.
2 P.W. Bridgman, Proc. Am. Acad. Arts Sci., 44 (1909) 201, 221, 255.
3 P.W. Bridgman, The Physics of High Pressure, G. Bell and Sons, London, 1952.
4 P.W. Bridgman, Rev. Mod. Phys., 18 (1946) 1.
5 P.W. Bridgman, Proc. Am. Acad. Arts Sci., 61 (1926) 67.
6 P.W. Bridgman, Proc. Am. Acad. Arts Sci., 72 (1926) 227.
7 P.W. Bridgman, Phys. Rev., 48 (1935) 825.
8 P.W. Bridgman, J. Am. Chem. Soc., 36 (1914) 1344.
9 P.W. Bridgman, J. Am. Chem. Soc., 38 (1916) 609.
10 P.W. Bridgman, Proc. Am. Acad. Arts Sci., 81 (1952) 169.
11 P.W. Bridgman, Phys. Rev., 48 (1935) 893.
12 P.W. Bridgman, Phys. Rev., 57 (1940) 342.
13 P.W. Bridgman, Phys. Rev., 48 (1935) 897.
14 P.W. Bridgman, J. Appl. Phys., 12 (1941) 461.
15 P.W. Bridgman, Proc. Roy. Soc., Ser. A, 203 (1950) 1.
16 P.W. Bridgman, Proc. Am. Acad. Arts Sci., 81 (1952) 165.
17 C.C. Bradley (Ed.), High Pressure Methods in Solid State Research, Plenum Press, New York, 1969.
18 R.H. Wentorf, Jr. (Ed.), Modern Very High Pressure Techniques, Butterworths, London, 1962; Advances in High Pressure Research, Vol. 4, Academic Press, New York, 1974.
19 W. Paul and D.M. Warschauer (Eds.), Solids under Pressure, McGraw-Hill, New York, 1963.
20 F.P. Bundy, W.R. Hibbard and H.M. Strong (Eds.), Progress in Very High Pressure Research, Wiley, New York, 1961.

21 R.S. Bradley (Ed.), High Pressure Physics and Chemistry, Vols. 1 and 2, Academic Press, New York, 1963; R.S. Bradley (Ed.), Advances in High-Pressure Research, Vols. 1—3, Academic Press, New York, 1966, 1969.
22 F. Seitz, D. Turnbull, and H. Ehrenreich (Eds.), Solid State Physics, Vols. 6, 1957; 13, 1962; 17, 1965; 19, 1966; Academic Press, New York.
23 S.D. Hamann, Physico-Chemical Effects of Pressure, Butterworths, London, 1959.
24 I.E. Weale, Chemical Reactions at High Pressure, E. and F.N. Spon, London, 1967.
25 L.S. Whatley and A. Van Valkenburg, in R.S. Bradley (Ed.), Advances in High Pressure Research, Academic Press, New York, 1966, p. 327.
26 E. Sinn, Coord. Chem. Rev., 12 (1974) 185, and references therein.
27 H.G. Drickamer and C.W. Frank, Electronic Transitions and the High Pressure Chemistry and Physics of Solids, Chapman and Hall, London, 1973, and references therein; H.G. Drickamer, Angew. Chem. Int. Ed. Engl., 13 (1974) 39; H.G. Drickamer, in W. Paul and D.M. Warschauer (Eds.), Solids Under Pressure, McGraw-Hill, New York, 1963, pp. 357—384.
28 J.R. Ferraro and L.J. Basile, Appl. Spectrosc., 28 (1974) 505.
29 S.D. Hamann, in R.S. Bradley (Ed.), Advances in High Pressure Research, Vol. 1, Academic Press, New York, 1966, p. 85; E.F. Green and J.P. Toennies, Chemical Reactions in Shock Waves, Arnold, London, 1964.
30 R.A. Fitch, T.E. Slykhouse and H.G. Drickamer, J. Opt. Soc. Am., 47 (1957) 1015.
31 E. Fishman and H.G. Drickamer, Anal. Chem., 28 (1956) 804.
32 H.G. Drickamer, in F.P. Bundy, W.R. Hibbard and H.M. Strong (Eds.), Progress in Very High Pressure Research, Wiley, New York, 1961, p. 16.
33 H.G. Drickamer and A.S. Balchan, in R.N. Wentorf (Ed.), Modern Very High Pressure Techniques, Butterworths, London, 1962, p. 25.
34 A.S. Balchan and H.G. Drickamer, Rev. Sci. Instrum., 31 (1960) 511.
35 W.F. Sherman, J. Sci. Instrum., 43 (1966) 462.
36 S.K. Runcorn, J. Appl. Phys., 27 (1956) 598.
37 Y.A. Klyuev, Inst. Exp. Techn., 5 (1964) 1.
38 R.P. Lowndes, Phys. Rev., B, 1 (1970) 2754.
39 K. Noack, Spectrochim. Acta, Part A, 24 (1968) 1917.
40 E. Peters and J.J. Byerley, Rev. Sci. Instrum., 34 (1963) 819.
41 E. Fishman and H.G. Drickamer, J. Chem. Phys., 24 (1956) 548.
42 C.S. Fang, J.V. Fox, C.E. Mauk and R.W. Prengle, Appl. Spectrosc., 24 (1970) 21.
43 H.W. Schamp, Rev. Sci. Instrum., 30 (1959) 1051.
44 S.J. Gill and W.D. Rummel, Rev. Sci. Instrum., 32 (1961) 756.
45 J.R. Ferraro, Raman Newsletter, No. 55, p. 17. July 1973.
46 M. Nicol, Y. Ebisuzaki, W.D. Ellenson and A. Karim, Rev. Sci. Instrum., 43 (1968) 1368.
47 F.P. Bundy, Rev. Sci. Instrum., 46 (1975) 1318.
48 C.E. Weir, E.R. Lippincott, A. Van Valkenburg and E.N. Bunting, J. Res. Nat. Bur. Stand., Sect. A, 63 (1959) 55; E.R. Lippincott, C.E. Weir, A. Van Valkenburg and E.N. Bunting, Spectrochim. Acta, 16 (1960) 58; E.R. Lippincott, F.E. Welsh, and C.E. Weir, Anal. Chem., 33 (1961) 137.
49 W.A. Bassett, T. Takahashi and P.W. Stook, Rev. Sci. Instrum., 38 (1967) 37.
50 J.R. Ferraro and A. Quattrochi, Appl. Spectrosc., 24 (1971) 102.
51 L. Ming and W.A. Bassett, Rev. Sci. Instrum., 45 (1974) 1115.
52 J.R. Ferraro and J. Takemoto, Appl. Spectrosc., 28 (1974) 66.
53 D.M. Adams, S.J. Payne and K. Martin, Appl. Spectrosc., 27 (1973) 377.
54 J.D. Barnett, S. Block and G.J. Piermarini, Rev. Sci. Instrum., 44 (1973) 1.
55 S. Block and G. Piermarini, Phys. Today, 29 (1976) 44.
56 H.K. Mao and P.M. Bell, Ann. Rep. Geophys. Lab., (1975—1976) 824.
57 P.M. Bell, Science, 200 (1978) 1145.

58 (a) E.R. Lippincott and H.C. Duecker, Science, 144 (1964) 1119. (b) H.C. Duecker and E.R. Lippincott, Doctoral Thesis, University of Maryland, College Park, 1964.
59 C. Postmus, V.A. Maroni and J.R. Ferraro, Inorg. Nucl. Chem. Lett., 4 (1968) 269.
60 J.W. Brasch and E.R. Lippincott, Chem. Phys. Lett., 2 (1968) 99.
61 A.J. Melveger, J.W. Brasch and E.R. Lippincott, Appl. Opt., 9 (1970) 11.
62 J.W. Brasch and R.J. Jakobsen, Spectrochim. Acta, 21 (1965) 1183.
63 J.W. Brasch, J. Chem. Phys., 43 (1965) 3473; R.J. Jakobsen, Y. Mikawa and J.W. Brasch, Appl. Spectrosc., 24 (1970) 333.
64 J.R. Ferraro, S.S. Mitra and C. Postmus, Inorg. Nucl. Chem. Lett., 2 (1966) 269.
65 C. Postmus, J.R. Ferraro and S.S. Mitra, Inorg. Nucl. Chem. Lett., 4 (1968) 155.
66 G.J. Long, G. Miles and J.R. Ferraro, Appl. Spectrosc., 28 (1974) 377.
67 N.T. McDevitt, R.E. Witkowski and W.C. Fateley, Abstr., 13th Colloquium Spectroscopium Internationale, June 18—24, 1967, Ottawa, Canada.
68 J.R. Ferraro, unpublished results.
69 J.R. Ferraro and L.J. Basile, Am. Lab., 11 (1979) 31.
70 C.C. Bradley, H.A. Gebbie, V.V. Kechin and J.H. King, Nature (London), 211 (1966) 839.
71 N.B. Owen, J. Sci. Instrum., 43 (1966) 765.
72 D.M. Adams and S.J. Payne, J. Chem. Soc. Faraday Trans., 70 (1974) 1959.
73 D.M. Adams and S.K. Sharma, J. Phys. E, 10 (1977) 838.
74 D.M. Adams, S.K. Sharma and R. Appleby, Appl. Opt. 16 (1977) 2572.
75 D.M. Adams and S.K. Sharma, J. Phys. E, 10 (1977) 680.
76 M.G. Gonikberg, K.H.E. Stein, S.A. Unkholin, A.A. Opekunov, and V.T. Aleksanias, Opt. Spectrosc., 6 (1959) 166.
77 W.B. Daniels and A.A. Hruschka, Rev. Sci. Instrum., 28 (1957) 1058.
78 W.B. Daniels, Rev. Sci. Instrum., 37 (1966) 1502.
79 O. Brafman, S.S. Mitra, R.K. Crawford, W.B. Daniels, C. Postmus, and J.R. Ferraro, Solid State Commun., 7 (1969) 449.
80 G.E. Walrafen, in A.K. Covington and P. Jones (Eds.), Hydrogen-Bonded Solvent Systems, Taylor and Francis, London, 1968, p. 9.
81 G.E. Walrafen, J. Solution Chem. 2 (1973) 159.
82 A.B. Davis and W.A. Adams, Spectrochim. Acta, Part A, 27 (1971) 2401.
83 J. Jean-Louis and H. Vu, Rev. Phys. Appl., 7 (1972) 89.
84 P.S. Peercy, Phys. Rev. Lett., 31 (1973) 379.
85 P.S. Peercy and G.A. Samara, Phys. Rev., B, 8 (1973) 2033.
86 G.A. Samara and P.S. Peercy, Phys. Rev., B, 7 (1973) 1131.
87 S.C. Durana and J.P. McTague, Phys. Rev. Lett., 31 (1973) 990.
88 P.T.T. Wong and E. Whalley, Rev. Sci. Instrum., 45 (1974) 904; 43 (1972) 935.
89 J.H. Campbell and J. Jonas, Chem. Phys. Lett., 18 (1973) 441.
90 H.K. Mao and P.M. Bell, Science, 191 (1976) 851.
91 P. Walling and J.R. Ferraro, Rev. Sci. Instrum., 49 (1978) 1557.
92 S. Foner, Rev. Sci. Instrum., 30 (1959) 548.
93 A.H. Ewald and E. Sinn, Inorg. Chem., 6 (1967) 40.
94 A.H. Ewald, R.L. Martin, I.G. Ross and A.H. White, Proc. Roy. Soc. Ser. A, 280 (1964) 235.
95 E. Sinn, Thesis, University of Sydney, 1966.
96 S. Broersma, Rev. Sci. Instrum., 34 (1963) 277.
97 D.B. McWhan and A.L. Stevens, Phys. Rev., A, 139 (1965) 682; L.H. Adams and J.W. Green, Phil. Mag., 12 (1931) 367.
98 D. Bloch, High Temp.-High Pressures, 1 (1969) 1.
99 K. Mori and M. Mayashi, J. Phys. Soc. Jpn., 33 (1972) 1396.
100 D.F. Evans, J. Chem. Soc., (1959) 2003.
101 R.V. Pound, G.B. Benedek and R. Drever, Phys. Rev. Lett., 7 (1961) 405.

102 M. Nicol and G. Jura, Science, 141 (1963) 1035.
103 D.N. Pipkorn, C.K. Edge, P. Debrunner, G. DePasquali, H.G. Drickamer and H. Frauenfelder, Phys. Rev., A, 135 (1964) 1604.
104 F.E. Huggins, H.K. Mao, and D. Virgo, Ann. Rep. Geophys. Lab., (1974—1975) 405.
105 G.B. Benedek, Magnetic Resonance at High Pressures, Interscience, New York, 1963.
106 T. Kushida, G.B. Benedek, and N. Bloembergen, Phys. Rev., 104 (1956) 1364.
107 J.D. Litster and G.B. Benedek, J. Appl. Phys., 34 (1963) 688.
108 I.P. Kaminov and R.V. Jones, Phys. Rev., 123 (1961) 1122.
109 W.M. Walsh, Phys. Rev., 122 (1961) 762.
110 G.D. Watkins and R.V. Pound, Phys. Rev., 89 (1953) 658.
111 W.M. Walsh, Phys. Rev., 114 (1959) 1485.
112 R.G. Shulman, 3.J. Wylaeda and P.W. Anderson, Phys. Rev., 107 (1957) 953.
113 U.V. Lemanov, Sov. Phys.-JETP, 13 (1961) 543.
114 T. Fuke, J. Phys. Soc. Jpn., 16 (1961) 266.
115 R.G. Barnes and R.D. Engardt, J. Chem. Phys., 29 (1958) 248.
116 D. Danthreppe and B. Dreyfus, C.R. Acad. Sci., 241 (1955) 795.
117 R.A. Bernheim and H.S. Gentowski, J. Chem. Phys., 32 (1960) 1072.
118 B.C. Giessen and G.E. Gordon, Science, 159 (1968) 973.
119 E.A. Perez-Albuerne and H.G. Drickamer, J. Chem. Phys., 43 (1965) 1381.
120 G.J. Piermarini and S. Block, Rev. Sci. Instrum., 46 (1975) 973.
121 W.A. Bassett and T. Takahashi, in R.H. Wentorf, Jr. (Ed.), Advances in High Pressure Research, Vol. 4, Academic Press, London, 1974.
122 R. Fourne, J. Appl. Crystallogr., 1 (1968) 23.
123 L. Merrill and W.A. Bassett, Rev. Sci. Instrum., 45 (1974) 290.
124 W. Denner, W. Dieterich, H. Schultz, R. Keller and W.B. Holzapfel, Rev. Sci. Instrum., 49 (1978) 775.
125 G.J. Piermarini, R.A. Forman and S. Block, Rev. Sci. Instrum., 49 (1978) 1061.
126 H.W. Davies, J. Res. Nat. Bur. Stand., Sect. A, 72 (1968) 149.
127 J.R. Ferraro, Inorg. Nucl. Chem. Lett., 6 (1970) 823.
128 J.R. Ferraro, D.W. Meek, E.C. Siwiec and A. Quattrochi, J. Am. Chem. Soc., 93 (1971) 3862.
129 R.A. Forman, G.J. Piermarini, J.D. Barnett and S. Block, Science, 176 (1972) 284.
130 G.J. Piermarini, S. Block and J.D. Barnett, J. Appl. Phys., 44 (1973) 5377.
131 R.A. Forman, B.A. Weinstein and G. Piermarini, Spectroscopie des Elements de Transition et des Elements Lourds dans les Solides, Edition du Centre National de la Recherche Scientifique, Lyon, France, 1977.
132 H.K. Mao and P.M. Bell, Ann. Rep. Geophys. Lab., (1975—1976) 509.
133 H.K. Mao, P.M. Bell, J.W. Shaner and D.J. Steinberg, J. Appl. Opt., 49 (1978) 3276.
134 H.K. Mao and P.M. Bell, Ann. Rep. Geophys. Lab., (1975—1976) 827.
135 H.K. Mao and P.M. Bell, Ann. Rep. Geophys. Lab., (1976—1977) 644, 650.
136 J.V. Fox and H.W. Prengle, Appl. Spectrosc., 23 (1969) 157.
137 D.L. Decker, W.A. Bassett, L. Merrill, H.T. Hall and J.D. Barnett, High Pressure Calibration — A Critical Review, High Pressure Data Center, Brigham Young University, Provo, Utah, 1973.
138 H.G. Drickamer and J.C. Zahner, in I. Prigogine (Ed.), Advances in Chemical Physics, Vol. IV, Interscience, New York, 1962, p. 161; W.T. Carnall, S. Siegel, J.R. Ferraro, B. Tani and E. Gebert, Inorg. Chem., 12 (1973) 560.
139 J.R. Ferraro, in C.N.R. Rao and J.R. Ferraro (Eds.), Spectroscopy in Inorganic Chemistry, Academic Press, New York, 1971, pp. 57—77.
140 D.M. Adams and R. Appleby, J. Chem. Soc. Dalton Trans., (1977) 1530.
141 D.M. Adams and R. Appleby, J. Chem. Soc. Dalton Trans., (1977) 1535.
142 D.M. Adams and R. Appleby, Inorg. Chim. Acta, 26 (1978) L43.
143 R.W.G. Wyckoff, Crystal Structures, Vol. 1, Interscience, New York, 1963, pp. 309—310.

144 J.D.H. Donnay and H.M. Ondik, Crystal Tables, Inorganic Compounds, Vol. 2, U.S. Dept. Commerce and Nat. Bur. Stand., 1973, p. 061.
145 Y. Mikawa, R.J. Jakobsen and J.W. Braasch, J. Chem. Phys., 45 (1966) 4528.
146 D.M. Adams and S.K. Sharma, J. Chem. Soc. Faraday Trans. 2, 74 (1978) 1355.
146a P.T.T. Wong, J. Chem. Phys., 70 (1979) 456.
147 D.M. Adams and S.K. Sharma, J. Chem. Soc. Faraday Trans. 2, 72 (1976) 1344.
148 D.M. Adams and S.K. Sharma, J. Chem. Soc. Faraday Trans. 2, 72 (1976) 848.
149 S.D. Cifrulak, Amer. Mineral., 55 (1970) S15.
150 M.Y. Fong and M. Nicol, J. Chem. Phys., 54 (1971) 579.
151 M. Nicol and W.D. Ellenson, J. Chem. Phys., 56 (1972) 677.
152 D.M. Adams and S.K. Sharma, Chem. Phys. Lett., 36 (1975) 407.
153 D.M. Adams and S.K. Sharma, J. Chem. Soc. Faraday Trans., 2, 74 (1978) 1355.
154 R. Blinc, J.R. Ferraro, and C. Postmus, J. Chem. Phys., 51 (1969) 732.
155 P.S. Peercy, Phys. Rev. Lett., 31 (1973) 379.
156 P.S. Peercy and G.A. Samara, Phys. Rev., B, 8 (1973) 2033.
157 M. Nicol and J.F. Durana, J. Chem. Phys., 54 (1971) 1436.
158 S.D. Hamann and M. Linton, Aust. J. Chem., 29 (1976) 479.
159 D. Greig, D.F. Shriver and J.R. Ferraro, J. Chem. Phys., 66 (1977) 5246.
160 R.C. Hanson, T.A. Fjeldly and H.D. Hochheimer, Phys. Status Solidi B, 70 (1975) 567.
161 D. Greig, G.C. Joy and D.F. Shriver, J. Electrochem. Soc., 123 (1976) 588.
162 P.T.T. Wong and E. Whalley, Rev. Sci. Instrum., 43 (1972) 935.
163 Y. Ebisuzaki and M. Nicol, Chem. Phys. Lett., 3 (1969) 480.
164 F.D. Medina and W.B. Daniels, J. Chem. Phys., 64 (1976) 150.
165 J.E. Bertie and E. Whalley, J. Chem. Phys., 40 (1964) 1646.
166 J.P. Marckmann and E. Whalley, J. Chem. Phys., 41 (1964) 1450.
167 J.R. Ferraro, in S. Nudelman and S.S. Mitra (Eds.), Far Infrared Properties of Solids, Plenum Press, New York, 1970, pp. 451—474.
168 D.W. Berreman, Phys. Rev., 130 (1963) 2193.
169 S.S. Mitra and P.J. Gielisse, AFCRL-69-395, June 1965.
170 C.M. Randall, R.M. Fuller and D.J. Montgomery, Solid State Commun., 2 (1964) 273.
171 C.L. Bottger and A.L. Geddes, J. Chem. Phys., 46 (1967) 3000.
172 H.G. Drickamer, R.W. Lynch, R.L. Clendenen and E.A. Perez-Albuerne, Adv. Solid State Phys., 19 (1966) 135.
173 R.L. Clendenen and H.G. Drickamer, J. Chem. Phys., 44 (1966) 4223.
174 S.S. Mitra, C. Postmus and J.R. Ferraro, Phys. Rev. Lett., 18 (1967) 455.
175 J.R. Jasperse, A. Kahan, J.N. Plendl and S.S. Mitra, Phys. Rev., 146 (1966) 526.
176 C. Postmus, J.R. Ferraro and S.S. Mitra, Phys. Rev., 174 (1968) 983.
177 M. Pagannone and H.G. Drickamer, J. Chem. Phys., 43 (1965) 2266.
178 C.F. Cline and D.R. Stephens, J. Appl. Phys., 36 (1965) 2869.
179 S.S. Mitra, Phys. Status Solidi, 9 (1965) 519.
180 M. Born and K. Huang, Dynamical Theory of Crystal Lattices, Oxford Univ. Press, London and New York, 1954, p. 52.
181 F. Seitz, Modern Theory of Solids, McGraw-Hill, New York, 1940, p. 80.
182 R.A. Cowley, Adv. Phys., 12 (1963) 421.
183 E.R. Cowley and R.A. Cowley, Proc. Roy. Soc., Ser. A, 287 (1965) 259.
184 S.S. Mitra and R. Marshall, J. Chem. Phys., 41 (1964) 3158.
185 J.R. Ferraro, C. Postmus, S.S. Mitra and C. Hoskins, Appl. Spectrosc., 24 (1970) 187.
186 C. Postmus, J.R. Ferraro, S.S. Mitra and C. Hoskins, Appl. Opt., 9 (1970) 5.
187 F. Fondere, J. Obriot and Ph. Marteau, J. Mol. Struct., 45 (1978) 89.
188 O. Brafman, S.S. Mitra, R.K. Crawford, W.B. Daniels, C. Postmus and J.R. Ferraro, Solid State Commun., 7 (1969) 449.

189 J.R. Ferraro, S.S. Mitra and A. Quattrochi, J. Appl. Phys., 42 (1971) 3677.
190 J.R. Ferraro, H. Horan and A. Quattrochi, J. Chem. Phys., 55 (1971) 664.
191 S.S. Mitra, Ind. J. Pure Appl. Phys., 9 (1971) 922.
192 C.J. Buchenauer, F. Cerdeira and M. Cardona, presented at the Second International Conference on Light Scattering of Solids, Paris, July 1971.
193 Y. Ebisuzaki and M. Nicol, J. Phys. Chem. Solids, 33 (1972) 763.
194 B.A. Weinstein and G.J. Piermarini, Phys. Lett. A, 48 (1974) 14; Phys. Rev., B, 12 (1975) 1172.
195 D.M. Adams and S.K. Sharma, J. Phys. Chem. Solids, 39 (1978) 515.
196 M. Nicol and M.Y. Fong, J. Chem. Phys., 54 (1971) 3167.
197 R.G. Pearson, J. Am. Chem. Soc., 91 (1969) 4947; J. Chem. Phys., 53 (1970) 2986; Pure and Appl. Chem., 27 (1971) 145. Symmetry Rules for General Reactions, Wiley, New York, 1976.
198 R.F.W. Bader, Can. J. Chem., 40 (1962) 1164; Mol. Phys., 3 (1960) 137.
199 R. Bayer and J.R. Ferraro, Inorg. Chem., 8 (1969) 1654.
200 P. Klaeboe and T. Woldbaek, Appl. Spectrosc., 32 (1978) 588.
201 F. Goetz, T.B. Brill and J.R. Ferraro, J. Phys. Chem., 82 (1978) 1912.
202 K. Nakamoto, C. Udovich, J.R. Ferraro, and A. Quattrochi, Appl. Spectrosc., 24 (1970) 606.
203 C. Postmus, K. Nakamoto and J.R. Ferraro, Inorg. Chem., 6 (1967) 2194.
204 C. Postmus, J.R. Ferraro, A. Quattrochi, K. Shobatake and K. Nakamoto, Inorg. Chem., 8 (1969) 1651.
204a A.B.P. Lever and B.S. Ramaswamy, Can. J. Chem., 51 (1973) 514; Spectrosc. Lett., 6 (1973) 67; M. Keeton, A.B.P. Lever and B.S. Ramaswamy, Spectrochim. Acta, 26A (1970) 2173.
205 D.M. Adams and S.J. Payne, Inorg. Chim. Acta, 19 (1976) L49.
206 J.R. Ferraro, J. Chem. Phys., 53 (1970) 117.
207 R.G. Dickinson, J. Am. Chem. Soc., 44 (1922) 2404.
208 D.M. Adams and S.J. Payne, J. Chem. Soc. Dalton Trans., (1974) 407.
209 D.M. Adams and S.J. Payne, J. Chem. Soc. Dalton Trans., (1975) 215.
210 G. Dehnicke, K. Dehnicke, H. Ahsbahs and E. Hellner, Ber. Bunsenges. Phys. Chem., 78 (1974) 1010.
211 D.M. Adams, J.D. Findlay and S.J. Payne, J. Chem. Soc. Dalton Trans., (1976) 371.
212 D.M. Adams, S.J. Payne and K. Martin, Appl. Spectrosc., 27 (1973) 377.
213 J.R. Ferraro, K. Nakamoto, J.T. Wang and L. Lauer, J. Chem. Soc., (1973) 266.
214 L. Sacconi and J.R. Ferraro, Inorg. Chim. Acta, 9 (1974) 49.
215 J.R. Ferraro and J. Takemoto, Appl. Spectrosc., 28 (1974) 66.
216 D.C. Fisher and H.G. Drickamer, J. Chem. Phys., 54 (1971) 4825.
217 R.J. Butcher, J.R. Ferraro and E. Sinn, Inorg. Chem., 15 (1976) 2077.
218 R.J. Butcher, J.R. Ferraro and E. Sinn, J. Chem. Soc. Chem. Commun., (1976) 910.
219 J.R. Ferraro and L. Fabbrizzi, Inorg. Chim. Acta, 26 (1978) 615.
220 E. Hellner, H. Ahsbahs, G. Dehnicke and K. Dehnicke, Naturwissenschaften, 61 (1974) 502.
221 S.C. Fung and H.G. Drickamer, Proc. Nat. Acad. Sci. U.S.A., 62 (1969) 38.
222 E. Hellner, H. Ahsbahs, G. Dehnicke and K. Dehnicke, Ber. Bunsenges. Phys. Chem., 77 (1973) 277.
223 J.R. Ferraro, D.W. Meek, E.C. Siwiec and A. Quattrochi, J. Am. Chem. Soc., 93 (1971) 3862.
224 H.G. Drickamer, Solid State Phys., 17 (1965) 1.
225 G.J. Long and J.R. Ferraro, Inorg. Nucl. Chem. Lett., 10 (1974) 393.
226 J.R. Ferraro and G.J. Long, Accounts Chem. Res., 8 (1975) 171.
227 G.J. Long and J.R. Ferraro, J. Chem. Soc. Chem. Commun., (1973) 719; G.J. Long and D.L. Coffen, Inorg. Chem., 13 (1974) 270.

228 R.W. Vaughan and H.G. Drickamer, J. Chem. Phys., 47 (1967) 468.
229 R.D. Willett, J.R. Ferraro and M. Choca, Inorg. Chem., 13 (1974) 2919.
230 P.J. Wang and H.G. Drickamer, J. Chem. Phys., 59 (1973) 559.
231 L.J. Basile, J.R. Ferraro, M. Choca and K. Nakamoto, Inorg. Chem., 13 (1974) 496.
232 C.B. Bargeron, M. Avinor and H.G. Drickamer, Inorg. Chem., 10 (1971) 1338.
233 C.B. Bargeron and H.G. Drickamer, J. Chem. Phys., 55 (1971) 3471.
234 C.W. Frank and H.G. Drickamer, J. Chem. Phys., 56 (1972) 3551.
235 P.J. Wang and H.G. Drickamer, J. Chem. Phys., 59 (1973) 713.
236 L.J. Basile, J.H. Enemark, R.D. Feltham, J.R. Ferraro and T.E. Nappier, unpublished data.
237 M.C. Browning, J.R. Mellor, D.J. Morgan, S.A.J. Pratt, L.E. Sutton and L.M. Vananzi, J. Chem. Soc., (1962) 693.
238 B.T. Kilbourn, H.M. Powell and J.A.C. Darbyshire, Proc. Chem. Soc., London, (1963) 207; B.T. Kilbourn and H.M. Powell, J. Chem. Soc. A, (1970) 1688.
239 G.J. Long and E.O. Schlemper, Inorg. Chem., 13 (1974) 279.
240 D.N. Anderson and R.G. Willett, Inorg. Chim. Acta, 8 (1974) 167.
241 K.N. Raymond, P.W.R. Corfield and J.A. Ibers, Inorg. Chem., 7 (1968) 1362.
242 J.R. Ferraro and K. Nakamoto, Inorg. Chem., 11 (1972) 2290.
243 A. Earnshaw, E.A. King and L.F. Larkworthy, J. Chem. Soc. A, (1969) 2459.
244 K.J. Haller, P.L. Johnson, R.D. Feltham, J.H. Enemark, J.R. Ferraro and L.J. Basile, Inorg. Chim. Acta, 33 (1979) 119.
245 C.P. Brock, J.P. Collman, G. Dolcetti, P.H. Farnham, J.A. Ibers, J.E. Lester and C.A. Reed, Inorg. Chem., 12 (1973) 1304.
246 J.S. Wood, Prog. Inorg. Chem., 16 (1972) 227.
247 S.C. Fung and H.G. Drickamer, J. Chem. Phys., 51 (1969) 4350, 4360.
248 J.R. Ferraro, unpublished data.
249 J.R. Ferraro, J. Coord. Chem., 5 (1976) 101.
250 R. Eisenberg and J.A. Ibers, J. Am. Chem. Soc., 87 (1965) 3776.
251 A.E. Smith, G.N. Schrauzer, V.P. Hayweg and W. Heinrich, J. Am. Chem. Soc., 87 (1965) 5798.
252 R. Eisenberg and H.B. Gray, Inorg. Chem., 6 (1967) 1844.
253 E.L. Muetterties, Accounts Chem. Res., 3 (1970) 266.
254 R.R. Holmes, Accounts Chem. Res., 5 (1972) 296.
255 E.L. Muetterties, Rec. Chem. Prog., 31 (1970) 51.
256 E.L. Muetterties and R.A. Schunn, Quart. Rev. (London), 20 (1966) 245.
257 E.L. Muetterties and C.M. Wright, Quart. Rev. (London), 21 (1967) 109.
258 L. Malatesta, M. Fermi and V. Valenti, Gazz. Chim. Ital., 94 (1964) 1278; E.B. Fleischer, A.E. Gebala, D.R. Swift and P.A. Tasker, Inorg. Chem., 11 (1972) 2775.
259 J.L. Hoard and J.V. Silverton, Inorg. Chem., 2 (1963) 235.
260 R.V. Parish, Coord. Chem. Rev., 1 (1966) 439.
261 F. Klanberg, D.R. Eaton, L.J. Guggenberger, and E.L. Muetterties, Inorg. Chem., 6 (1967) 1271.
262 S.J. Lippard, Prog. Inorg. Chem., 8 (1966) 109; R.V. Parish and P.G. Perkins, J. Chem. Soc., (1967) 345.
263 E.L. Muetterties, Inorg. Chem., 12 (1973) 1963.
264 H.H. Claassen, E.L. Gasner and H. Selig, J. Chem. Phys., 49 (1968) 1803.
265 G.R. Rossman, F.D. Tsay and H.B. Gray, Inorg. Chem., 12 (1973) 824.
266 J.L. Hoard, T.A. Hamor and M.D. Glick, J. Am. Chem. Soc., 90 (1968) 3172.
267 K.O. Hartman and F.A. Miller, Spectrochim. Acta, 24 (1968) 669.
268 B.R. McGarvey, Inorg. Chem., 5 (1966) 476.
269 R.G. Hayes, J. Chem. Phys., 44 (1966) 2210.
270 J.R. Ferraro, L.J. Basile, L.R. Garcia-Inequez, P. Paoletti and L. Fabbrizzi, Inorg. Chem., 15 (1976) 2342.
271 J.R. Ferraro, L. Fabbrizzi and P. Paoletti, Inorg. Chem., 16 (1977) 2127.

217a A.B.P. Lever, E. Mantovani and J.C. Donini, Inorg. Chem., 10 (1971) 2424; B.P. Kennedy and A.B.P. Lever, J. Am. Chem. Soc., 95 (1973) 6907.
272 J.R. Ferraro and A. Sherren, Inorg. Chem., 17 (1978) 2498.
273 J.R. Ferraro and L.J. Basile, unpublished data.
274 F. Birch, in W. Paul and D.M. Warschauer (Eds.), Solids Under Pressure, McGraw-Hill, New York, 1963, pp. 137—162, and references therein.
275 H.S. Yoder, Trans. Am. Geophys. Union, 31 (1950) 827.
276 G.J.F. MacDonald, Am. J. Sci., 254 (1956) 713.
277 F. Dachille and R. Roy, Z. Kristallogr. Kristallgeometrie, Kristallphys., Kristallchem., 111 (1959) 451.
278 F.R. Boyd and J.L. England, J. Geophys. Res., 65 (1960) 749.
279 S.P. Clark, E.C. Robertson and F. Birch, Am. J. Sci., 255 (1957) 628.
280 E.C. Robertson, F. Birch and G. MacDonald, Am. J. Sci., 255 (1957) 115.
281 F. Birch and P. LeCompte, Am. J. Sci., 258 (1960) 209.
282 A.E. Ringwood, Bull. Geol. Soc. Am., 69 (1958) 129.
283 F.R. Boyd and J.L. England, Minerals of the Mantle, Yearbook, Vol. 59 Carnegie Institute, Washington, D.C., 1960, p. 47.
284 A.E. Ringwood and A. Major, Earth Planet. Sci. Lett., 1 (1966) 135.
285 A.E. Ringwood and A. Major, Earth Planet. Sci. Lett., 1 (1966) 351; 5 (1968) 76.
286 S. Akimoto and Y. Syono, Phys. Earth Planet. Inter., 3 (1970) 186.
287 E. Ito, T. Matsumoto, K. Suito and N. Kawai, Proc. Jap. Acad., 48 (1972) 412.
288 W.A. Bassett and T. Takahashi, Trans. Am. Geophys. Union, 51 (1970) 841.
289 H.K. Mao and P.M. Bell, Annu. Rep., Geophys. Lab., Carnegie Institute, Washington, D.C., 1971, p. 176.
290 A.E. Ringwood, Geochim. Cosmochim. Acta, 15 (1958) 195; 26 (1962) 457; Nature (London), 198 (1963) 79.
291 C.B. Slar and L.C. Carrison, Geol. Soc. Am., Special Paper 101, (1967), p. 195; Trans. Am. Geophys. Union, 47 (1966) 207.
292 A.E. Ringwood and A. Major, Earth Planet. Sci. Lett., 1 (1966) 241.
293 S. Akimoto and H. Fujisawa, J. Geophys. Res., 73 (1968) 1467.
294 N. Kawai, S. Endo and K. Ito, Phys. Earth Planet. Inter., 3 (1970) 182.
295 M. Kumazawa, H. Sawamoto, E. Ohtani and K. Masaki, Nature (London), 247 (1974) 356.
296 L. Ming and W.A. Bassett, Science, 187 (1975) 66.
297 P.M. Bell, H.K. Mao, R.A. Weeks and A. Van Valkenburg, Annu. Rep., Geophys. Lab., Carnegie Institute, Washington, D.C. 1975—1976, pp. 515—520.
298 R.M. Hazen and C.T. Prewitt, Am. Mineral., 62 (1977) 309.
299 R.M. Hazen, Phys. Chem. Minerals, 1 (1977) 83.
300 R.M. Hazen and L.W. Finger, Science, 201 (1978) 1122.
301 R.M. Hazen, Am. Mineral., 62 (1977) 528.
302 R.M. Hazen, Science, 194 (1976) 105.
303 A.L. Hammond, Science, 190 (1975) 967.
304 A.E. Ringwood, Composition and Petrology of the Earth's Mantle, McGraw-Hill, New York, 1975, and references therein.
305 Industrial Research Development, May 1978, p. 35.
306 R.A. Kerr, Science, 201 (1978) 429.
307 H.K. Mao and P.M. Bell, Science, 200 (1978) 1145.
308 R.B. Sosman, The Properties of Silica, Chem. Catalog Co., New York, 1927.
309 P.W. Bridgman, Proc. Am. Acad. Arts Sci., 76 (1948) 55.
310 A.M. Benson and H.G. Drickamer, J. Chem. Phys., 27 (1957) 1164.
311 R.R. Wiederkelr and H.G. Drickamer, J. Chem. Phys., 28 (1958) 311.
312 T.M.K. Nedungadi, Proc. Ind. Acad. Sci. Sect. A, 11 (1940) 86.
313 J.F. Asell and M. Nicol, J. Chem. Phys., 49 (1968) 5395.
314 A.S. Davydov, Theory of Molecular Excitons, McGraw-Hill, New York, 1966.

315 H. Vu, R. Atwood and E. Staude, C. R. Acad. Sci., Paris, 257 (1963) 1771.
316 M.M. Jean-Louis, M. Bahreini, and H. Vu, C. R. Acad. Sci., Ser. B, 268 (1969) 47.
317 V. Gutmann and H. Mayer, Structure and Bonding, Vol. 31, Springer-Verlag, New York, 1976, pp. 49—66.
318 R. Kronig, J. de Boer and J. Korringa, Physica (Utrecht), 12 (1946) 245.
319 A.A. Abrikosov, Astron. Zh., 31 (1954) 112.
320 Y. Yakovlev, New Scientist, September 2, 1976, pp. 478—479.
321 A.L. Ruoff, in C.W. Chu and J.A. Woollam (Eds.), High-Pressure and Low-Temperature Physics, Plenum Press, New York, 1978, pp. 1—20.
322 A.K. McMahan, in C.W. Chu and J.A. Woollam (Eds.), High-Pressure and Low-Temperature Physics, Plenum Press, New York, 1978, pp. 21—42.
323 P.M. Bell and H.K. Mao, Ind. Res. Dev., April (1979) 57; Chem. Eng. News, March 5 (1979) 6; Science, 203 (1979) 1004.
324 A.L. Ruoff and D.A. Nelson, Chem. Eng. News, November 20, 1978, 22.